The Thesis Committee for Nawel Boumerdassi
Certifies that this is the approved version of the following thesis:

Molecular Dynamics simulations of multiple Ag nanoclusters deposition on a substrate

APPROVED BY
SUPERVISING COMMITTEE:

Supervisor: _____
Michael F. Becker

_____
Desidario Kovar

Molecular Dynamics simulations of multiple Ag nanoclusters deposition on a substrate

by

Nawel Boumerdassi, B.S.

Thesis

Presented to the Faculty of the Graduate School of
The University of Texas at Austin
in Partial Fulfillment
of the Requirements
for the Degree of

Master of Science in Engineering

The University of Texas at Austin
May 2014

Dedication

To my dear family.

Acknowledgements

I would like to start by expressing my sincere thanks to Dr. Michael F. Becker who has been my supervisor for these past two years. His acceptance of my Master of Science application in Electrical and Computer Engineering has definitely marked my career path and I am proud of the knowledge I learned thanks to his decision. I am very grateful for all the support and guidance that he provided to me during these past two years, making my international studies experience extremely varied, interesting and rewarding.

I would like also to thank the LAMA research group for sharing their knowledge and experience, especially Dr. Desidario Kovar, Dr. Keito, Guillaume Noiseau, Michael Gammage, and Jean-Gil Gutierrez. The time they spent with me in lab explaining to me the hands-on tools have been very helpful and the suggestions they made during our weekly research meetings have been very useful for my progress.

Finally, I would like to thank Melanie Gulick, Susanne Graves and Barry Levitch from the Graduate Advisory Office for their responsiveness and availability to help me out throughout my administrative paperwork. The deadlines of this prestigious degree are strict and they did a great job to make me meet them.

Abstract

Molecular Dynamics simulations of multiple Ag nanoclusters deposition on a substrate

Nawel Boumerdassi, M.S.E

The University of Texas at Austin, 2014

Supervisor: Michael Becker

Ag thin and thick films have been experimentally deposited using a technique called Laser Ablation of a Microparticle Aerosol (LAMA). This technique is based on a supersonic jet accelerating NPs of a few nm diameter up to 1000 m/s and operating at room temperature. The deposited films have experimentally demonstrated interesting properties such as dense growth with good adherence on the substrate. Aerosol feed rates have been fixed to 10 mg/h which corresponds to rate depositions of 10^{10} to 10^{11} NPs/s/cm^2. In order to model this deposition technique and possibly be able to predict the morphology and structure of deposited films using computational methods, we have designed MD programs simulating the depositions of several Ag nanoclusters onto a substrate at a fixed temperature (300 K). The variation of parameters such as cluster size, cluster impact energy, and deposition rate has influenced the morphology and structure of the deposited films. Cluster diameters have been set to 3 nm or 5 nm, cluster velocities set to 200 m/s (0.022 eV/atom), 400 m/s (0.069 eV/ atom), or 800 m/s (0.358 eV/atom), and the deposition rate adjusted to ensure relaxation times between impactions of 5 ps to 20 ps. The evolution of deposited film density, adherence, and crystal arrangement has been analyzed with the variation of the aforementioned parameters. The highest cluster velocities have enabled the deposition of smoother, denser, and more adherent films. NCs with an initial velocity of 200 m/s have shown ratios of flattening equal to 50 % as opposed to 85% flattening for NCs deposited at 800 m/s. These observations have enabled us to draw qualitative conclusions on the film density The deposited films are less porous when the cluster impaction velocity increases. Atomic mixing between substrate and impacted NC atoms increased with increasing deposition velocity, which can perhaps be correlated to an increase of adherence, assuming that more mixing will create stronger molecular binding in the cluster-substrate interaction. Finally, complete epitaxial growth was observed for the highest impaction velocities only, which indicates that recrystalization can occur for this range of impact energies (0.3 eV/atom - 0.5 eV/atom). Although experimental results have given more quantitative data on film density and sticking ratios, they agree with our modeling, and this comparison allows us to validate our MD simulations. However, some limitations have been faced, mainly because of long computing time requirements that a single laptop computer has not been able to support.

Table of Contents

List of Tables

List of Figures

Chapter 1: Introduction

1.1. Introduction to film growth

The understanding of film deposition has received significant attention because of its wide range of applications in semiconductors, micro-electronic devices, optical coatings, optoelectronic devices, magnetic materials, and organic materials. In particular, it is of paramount importance in coating technologies where it is used to cover other materials and either enhance already existing properties of said materials, or introducing new properties. The properties of the deposited films depend on their composition and microstructure and the ability to tailor their growth mechanism has been a key driving force in the nanoparticle assembly field.

An emphasis is placed on metallic nanoparticles in this work because of their many desirable mechanical properties [2]. More precisely, silver nanoparticles have certain remarkable attributes including high hardness and stable conductivity that have been widely explored these past decades. Such properties combined with their ability to be deposited as thin and thick films, make silver nanoparticles particularly interesting for Micro Electro-Mechanical Systems (MEMS) devices, some of which are already available on the market.

The porosity of a film is defined as the volume ratio between metal phase and voids. Deposition conditions can considerably alter the porosity of a film from the original bulk material and therefore have an impact on the film properties. In this context, the optical properties of porous silver thin films appear to be tunable, allowing high reflection and low absorption under certain deposition conditions [4], which has given rise to a wide range of applications in glazing units for building construction, automobiles, and solar energy devices for passive heat gain [3].

1.2. Metallic nanocluster deposition

1.2.1. Definition of nanoclusters

Nanoclusters (NCs) are small aggregates of atoms with a size varying from 1-100 nm. They are formed by a replication of the same sub-unit within its structure, e.g. an atom of a given element is replicated according its crystal structure. Their chemical composition and structure is exactly defined, as opposed to nanoparticles (NPs), which is often given with an approximate

size distribution and which may be polycrystalline. NCs size and shape are the governing factors of their properties. Such properties can be different than the corresponding bulk material properties. For example, the case of a bulk metal with well-known properties like high electrical and thermal conductivity, light reflectivity, mechanical ductility may show partially or completely different properties in metal NCs [1].

1.2.2. Towards film growth

As an alternative to conventional deposition techniques, which consist of heating the substrate up to hundreds of degrees Kelvin above room temperature to successfully grow thin films, energetic cluster impact (ECI) is based on the deposition of NCs with high kinetic energy on a substrate at room temperature [8] and can be used to deposit thin or thick films.

The most effective method of studying the interaction of a single NC on smooth surfaces as it impacts is by Molecular Dynamics computer simulation (MD). MD treats the system on an atomic level and does not involve phenomenological parameters. The deposition of metallic NPs to form an ordered film structure remains a difficult challenge and MD simulations could point out promising directions and help guide new measurements.

Various research studies have simulated the impact of NCs on a substrate using MD simulations. Among the various subjects of those papers were: interactions of Co clusters on an Al substrate using MD simulation [5]. The purpose was to study the number of disordered atoms and the film flatness on a substrate at fixed temperature (300 - 500 K) by depositing clusters of different velocity (100 up to 800 m/s) and different cluster sizes (55, 70, and 100 atoms) as shown in Figure 1. The results have shown that the shape of thin films is linearly dependent on the clusters' size and velocity. The thin films become flatter with an increase in velocity and surface roughness decreases. Moreover, the number of disordered atoms grows when the clusters' size and temperature become larger.

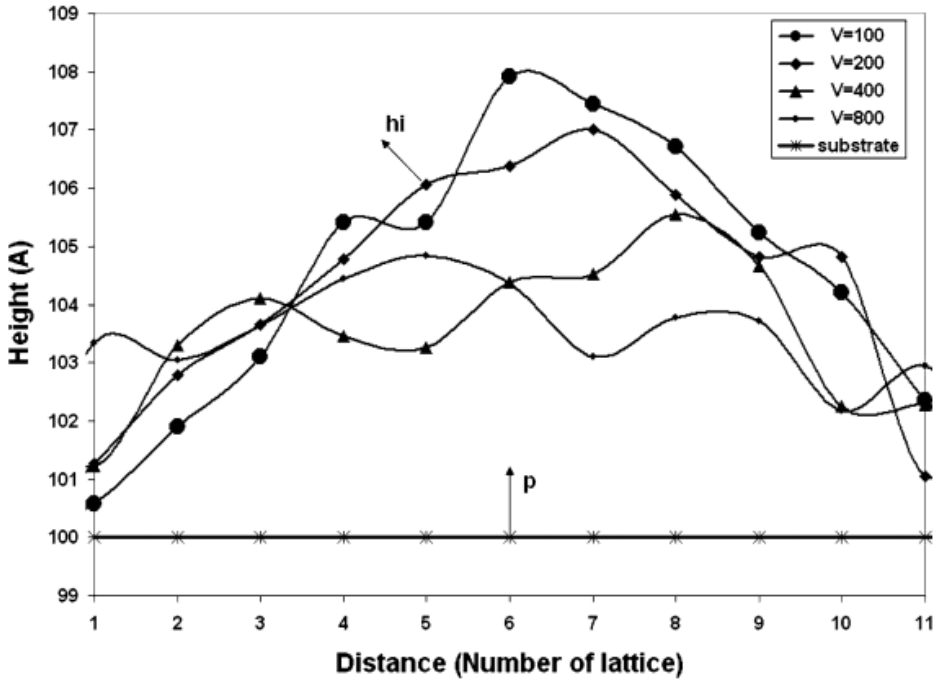

Figure 1: Surface section of a deposited cluster of 70 atoms. Figure taken from ref [5].

The parameters controlled included cluster size and composition and deposition conditions such as cluster kinetic energy. The main purpose of this fundamental research was to be able to predict the structure and morphology of the films given a set of deposition conditions. A good understanding of the cluster-surface interactions was a prerequisite to successfully achieve this goal.

Several studies on epitaxial growth of thin films have been published, and one of particular interest by Haberland, Insepov and Moseler [7] has identified the specific deposition conditions under which an epitaxial alignment occurs. The consecutive deposition of 50 Mo clusters (of 1045 atoms) onto a Mo surface at T=300 K was simulated for the three-impact energies: 0.1 eV/atom, 1 eV/atom and 10 eV/atom. The increase of the deposition energy leads to a change in film morphology from a porous film with multiple voids to a dense epitaxial film with a nearly bulk density (Figure 2).

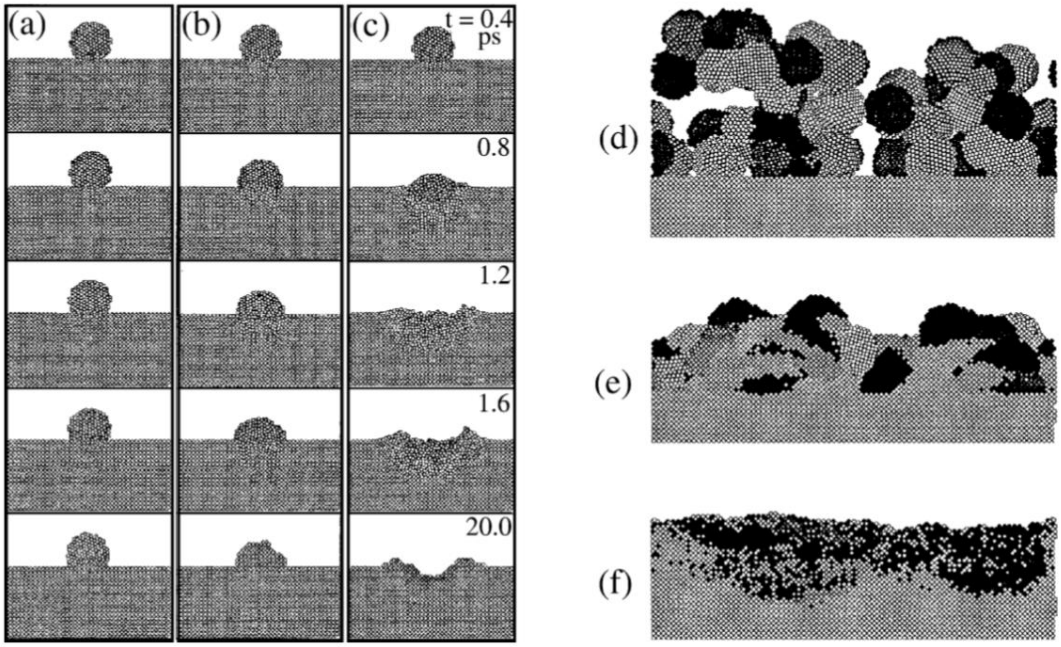

Figure 2: Molecular dynamics simulations of the impaction of Mo clusters on a Mo substrate. Snapshots of the morphology of cluster-assembled films deposited (a,d) 0.1 eV/atom; (b,e) 1 eV/atom; (c,f) 10 eV/atom. Taken from [7].

To summarize, high-energy NC deposition allows an epitaxial growth of the resulting thin films, with a smaller number of localized voids and a higher overall density. More porous and disordered structures of thin films have been measured with low-energy deposition, even when epitaxial growth can be observed. Right after the cluster hits the impaction zone, the surrounding atoms are given activation energy. The more disordered cluster atoms there are, the more chances that epitaxial growth can occur, assuming the relaxation time is long enough. It has been shown that the relaxation time of atoms is about 2 ps [6].

1.2.3. Cluster film morphology and structure

The morphology of thin films depends on material and temperature properties of both clusters and substrate and on the deposition energy of clusters. Harbich has experimentally distinguished three different regimes, i.e. low energy (~0.1 eV/atom), medium energy (1–10 eV/atom) and high energy (>10 eV/atom) deposition [10]. Low-energy deposition produces films

with a weak adherence to the substrate, and at medium energies the adherence increases and the film is colored, while high-energy deposition gives a hard shiny metallic coating.

In the general case, the impaction event for a single cluster has five possible distinct outcomes, which validates the previously stated observations: (i) deposition into a non-epitaxial configuration, (ii) deposition into an epitaxial configuration, (iii) crater formation by liquid flow, (iv) crater formation by hydrostatic pressure, (v) implantation. A review publication by Nordlund *et al.* [9] has been able to plot a phase diagram figure of the possible outcomes as shown in Figure 3, spanning a broad range of energy deposition (from 10 meV/atom to several MeV/cluster) and cluster sizes (1–300 000 atoms/cluster). In our work, we will restrict the simulation to the study of the boundary between epitaxial and non-epitaxial deposition because these regimes are basically the only ones that we can observe experimentally.

According to this diagram for Au NCs (assuming that results can be extrapolated to Ag clusters), very low energy and moderate-to-large cluster size deposition is most likely to remain in a non-epitaxial configuration after the impact. This is because it is unlikely the cluster would be perfectly aligned with the substrate on impact. On the other hand, for small cluster size and higher kinetic energy deposition, partly or fully epitaxial configuration might be observed. For our simulations, it is important to keep in mind that the transition from non-epitaxial to epitaxial growth is most likely to occur if the deposited clusters are below an upper bound in size or above a lower bound in kinetic energy.

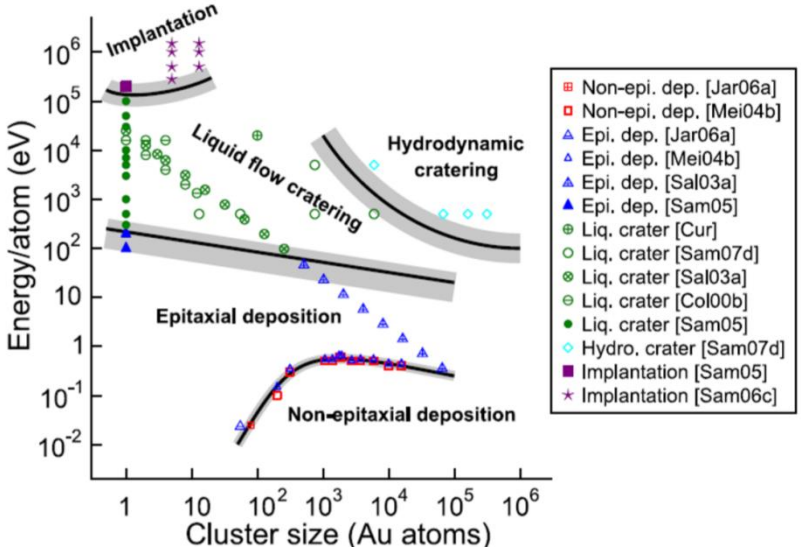

Figure 3: Diagram of the five possible outcomes after a cluster impact event. Taken from [9]

1.3. EXPERIMENTAL DEPOSITION USING LAMA PROCESS

The laser ablation of a microparticle aerosol (LAMA) process is a deposition technique capable of producing NPs from a wide variety of inorganic materials with a controllable size. It can be coupled with supersonic jet deposition to quickly direct-write nanostructured films with a thickness range of 1-100 micrometrers under gentle deposition conditions for the substrate [16].

Many of its aspects have been investigated, such as the supersonic acceleration of nanoparticles within an expanding background gas and the effect of background gas on the size and impacting energy of NPs (Huang *et al.* [14]), and the influence of the feedstock aerosol density on the agglomeration dynamics of NPs (Gleason *et al.* [11]). This system has also been tested with various starting feedstock materials, such as metals and ceramics. Finally, low temperature sintering, grain growth, and conductivity of nanoparticulate silver lines have been studied by Huang [14], Nahar [15] and Noiseau [13].

Figure 4 shows its experimental set-up that is based on the conversion of an aerosol of microparticles into an aerosol of nanoparticles by generating a laser breakdown-induced shockwave within the microparticles using a pulsed KrF excimer laser (λ = 248nm, 200Hz rep. rate) with 10 ns pulse width focused to fluences between 2–9 J/cm. The first step in LAMA is to generate an aerosol of MPs and direct it to the ablation chamber. The laser beam is monitored and focused on the ablation zone using a combination of lenses. The correct range of laser fluence enables converting the aerosol of MPs into an aerosol of NPs. The outgoing mostly NP aerosol then traverses a virtual impactor, which eliminates particles with a diameter larger than 0.5 micrometers. These particles could be either unablated microparticles or agglomerated NPs. Finally, the aerosol of NPs is accelerated to high velocity through flat-plate nozzle with a 250 μm – 1 mm orifice and directed onto a translating substrate to write patterned films. A pressure differential is created maintaining 1 atm pressure upstream of the nozzle and pumping to 200 mTorr in the direct-write chamber (downstream of the nozzle). This configuration produces an impaction velocity of approximately 1000 m/s for Ag NPs. [17]

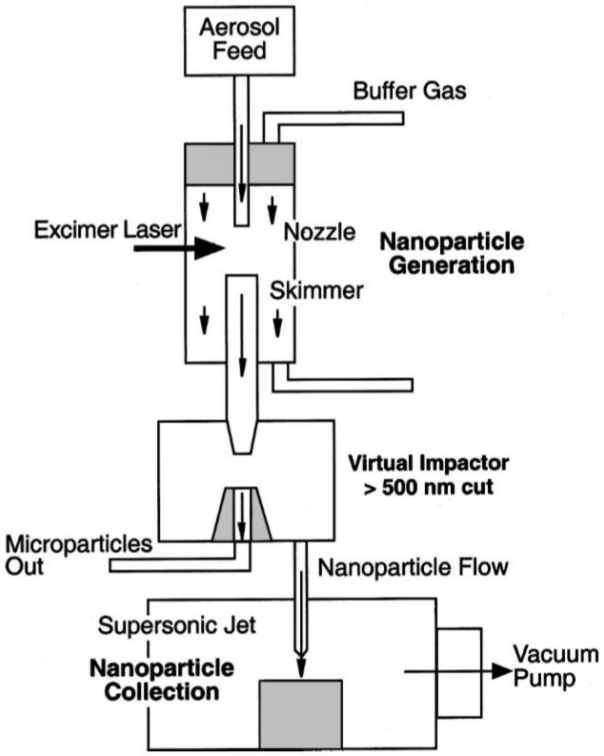

Figure 4: General scheme of Laser Ablation Molecular Aerosol (LAMA) experimental set-up. Taken from [17]

As shown in Figure 5, the impaction velocity of NPs varies in the range of 300-1200 m/s in argon and helium carrier gases and the mean NP sizes are between 5 and 10 nm with the smallest and fastest particles being formed in helium [14]. These impaction velocities correspond to impaction energies less than 1.0 eV/atom (Figure 6) for all but smallest NPs. These results suggest that supersonic jet deposition of NPs is a promising technique for the production of nanomaterials because such small NPs have a higher surface energy as compared to the surfaces of bulk materials, and thus densification and sintering processes may occur at or near room temperature during deposition.

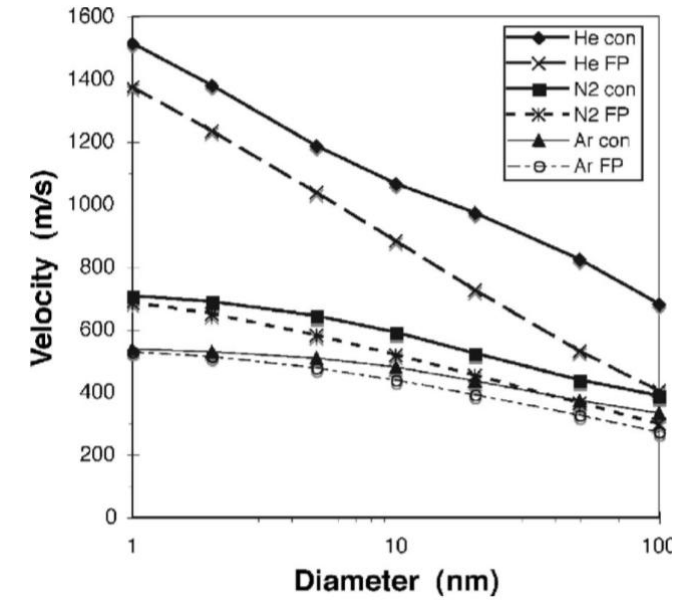

Figure 5: Evolution of the final NP velocity in the jet function of NP diameter, carrier gas, nozzle type. Nozzle diameter is 250 microns in all cases. Taken from [14].

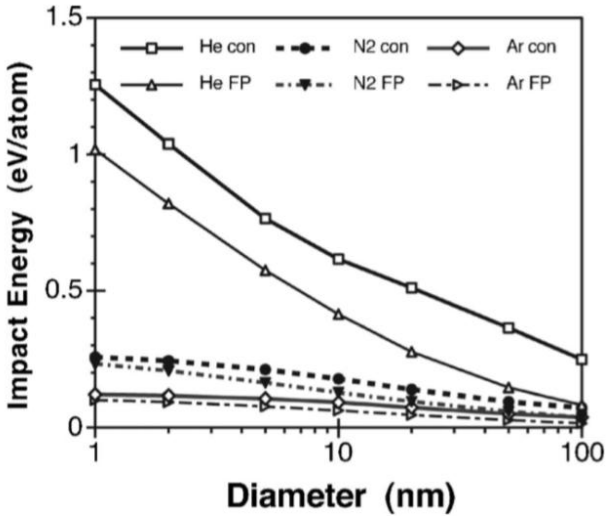

Figure 6: Evolution of NP impaction energy function of NP diameter, carrier gas, nozzle type. Nozzle-to-substrate distance is 2 mm. Taken from [14].

Our work is more oriented towards the understanding of NP deposition as opposed to NP synthesis with the LAMA process. For this reason, we will not go into a detailed description of the different theories developed on steps that occur before the deposition. However, it is

important to describe the calculations of NP velocity once they pass through the flat-plate nozzle (represented in Figure 7) to be able to compare our simulation results with relevant experimental data for cases for which they are available.

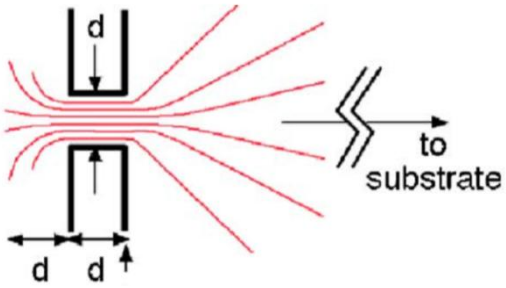

Figure 7: Flat-plate nozzle for supersonic jet impaction of NPs on a substrate. Taken from [14].

A model of the final velocity of the NPs near the axis of the jet as they impact onto the deposition surface has been developed. The throat velocity of the jet is limited at large pressure ratios to the choked flow velocity. For a flat-plate nozzle, the choked flow velocity at the exit is given by [14]:

$v_{\text{chocked}} = \sqrt{\frac{2\gamma}{(\gamma+1)} \frac{kT_0}{M_a}}$, where γ is the ratio of specific heats for the carrier gas (C_p/C_v), k is Boltzman's constant, T_o is the stagnation gas temperature, and M_a is the molecular mass of the gas. After travelling approximately 10 nozzle diameters, the jet in the free expansion reaches a an asymptotic velocity called v_{max} given by $v_{max} = \sqrt{\frac{2\gamma}{(\gamma-1)} \frac{kT_0}{M_a}}$.

The experimental measurements have shown that the NP final velocity is actually lower than the maximum expanded gas jet velocity when using flat-plate nozzles because the considerable drop of the gas density, pressure, and temperature in the first few nozzle diameters causes a drop in drag and acceleration. The flow parameters for the gases are summarized in Table I, and the velocities for He are notably larger than for the other gases due to its low molecular weight, indicating that He may be capable of accelerating the NP aerosol to the highest impaction velocity. Finally, the impaction energy in eV/atom for the impacting NPs is calculated and summarized in Table II. The impaction energy for He is higher within the range of 0.5 - 1.0 eV/atom. For the other gases, the impaction is softer with energies in the 0.05 - 0.25 eV/atom range [14].

Table I: Analytical and measured gas conditions given the stated flow parameters for three different gases. Taken from [14]

Parameter	Units	Helium	Nitrogen	Argon
Stagnation conditions				
T stag.	°C	300	300	300
Pressure stag.	Pa	1.01×10^5	1.01×10^5	1.01×10^5
Density stag.	kg/m^3	0.162	1.13	1.62
v sound	m/s	1019	353	323
v max	m/s	1766	790	559
Choked conditions				
T choked	°C	225	250	225
Pressure choked	Pa	4.92×10^4	5.34×10^4	4.92×10^4
Density choked	kg/m^3	0.105	0.719	1.05
v choked	m/s	883	322	279

Table II: Numerically calculated and experimentally measured parameters: mean mass-weighted NP diameter, impaction velocity and impaction energy of individual Ag nanoparticles, as well as deposited film grain size as a function of gas type and nozzle type. Taken from [14]

Gas type	Nozzle type	Mass-weighted NP diam (nm)	v impact (m/s)	E impact (eV/atom)	Scherrer size (nm) from (111)
He	FP	6.1	1020	0.58	14.4
He	Conical	6.1	1170	0.77	11.4
Ar	FP	15.8	320	0.057	23.6
Ar	Conical	15.8	380	0.081	20.3

1.4. SCOPE OF THIS WORK AND MOTIVATION

Molecular dynamics simulations appear to be a reliable technique to predict or confirm the morphology and structures of deposited thin films. The LAMA process has been used to deposit thin films, and numerous previous experiments have focused on the deposition of Ag NPs and the characterization of the resulting films. In order to correlate and confirm our molecular dynamics simulations with this experimental work, a computational modeling program has been designed in this work to simulate the deposition of Ag NCs on a substrate.

This work is divided in 3 different milestones: first, in the context of LAMA deposition experiments, relevant experimental conditions that can be modeled need to be identified concerning the deposition rate, the NPs size and the deposition velocity. Secondly, the effects of varying energy cluster deposition, cluster size, and substrate temperature on the microstructure of deposited thin films are simulated using a Molecular Dynamics (MD) approach. Finally, a measurement of film densities and an analysis of the crystal lattice at the cluster-substrate interface depending on deposition conditions using a MD tool is reported and compared to the experimental data from LAMA deposition results.

Experimental research using the LAMA technique has identified three different types of nanoparticles-substrate interaction after the impact event. Either the NPs are not accelerated enough to stick on the substrate and bounce-off, or they have a good adhesion and they grow thin films in epitaxial or non-epitaxial configurations. Given these experimental observations, the epitaxial to non-epitaxial boundary is investigated in this work, which limits the range of cluster size to a few nanometers and the range of energy deposition to 0.1 eV/atom to 10 eV/atom. In addition, simulations could help to guide the experiments towards epitaxial thin film deposition.

Chapter 2: Computational modeling tools

2.1. MOLECULAR DYNAMICS

MD is a widely used computational tool for modeling at the atomistic level complex problems in research areas such as chemistry, thermodynamics, and several other areas [18]. The basic idea of molecular dynamics is to calculate the forces, potential energy, velocities, and positions of the particles investigated given their initial state, and be able to observe their dynamical evolution. The most common method involves numerically solving the Newton equations of motion for a given system of many-body interactions, where the potential energy and forces between the particles are defined by molecular mechanical force fields. Once the trajectories of these particles are known, various global system properties as statistical average computations can be set and extracted.

MD simulations have the ability to model short periods of time and small distances in the range of Angstroms to nanometers for the length-scale, and events of femtoseconds to a few picoseconds for the time-scale. Both of these scales are extremely useful in the study of epitaxial growth [19]. However, MD calculation spends the major part of its computational time finding the atomic neighbor positions in order to evaluate the interatomic forces, and this computationally intensive calculation must be repeated for every time-step. This makes this technique extremely computationally expensive. As a result, serial MD simulations are usually applied to small systems up to a few thousands of atoms and for short periods of real deposition time up to a few picoseconds. This necessarily restricts both the numbers of atoms in the sample and the simulated time in order to make the computation practicable. This reduced time produces simulated conditions that might be seen in real world experience such as NP impaction physics.

Using a MD simulation entails making some choices. The most important choices include the choice of an adequate potential function to model the particles' interactions in the investigated problem, the option of a time integrator algorithm, the choice of periodic boundary conditions applied on the system to simplify the modeling and optimize the computation time, and the choice of statistical constraints, such as constant temperature imposed on the system. Each of these various options will be explained in detail in later sections. In particular, parameters that were used in this project will be emphasized. A schematic diagram in Figure 8 summarizes the sequence of steps of MD simulations, starting with the determination of force

fields at a given time step, moving the positions the particles through a time integrator with a certain velocity, setting a thermostat, computing the trajectories of the atoms, incrementing the time step and restarting the process until the simulation terminates.

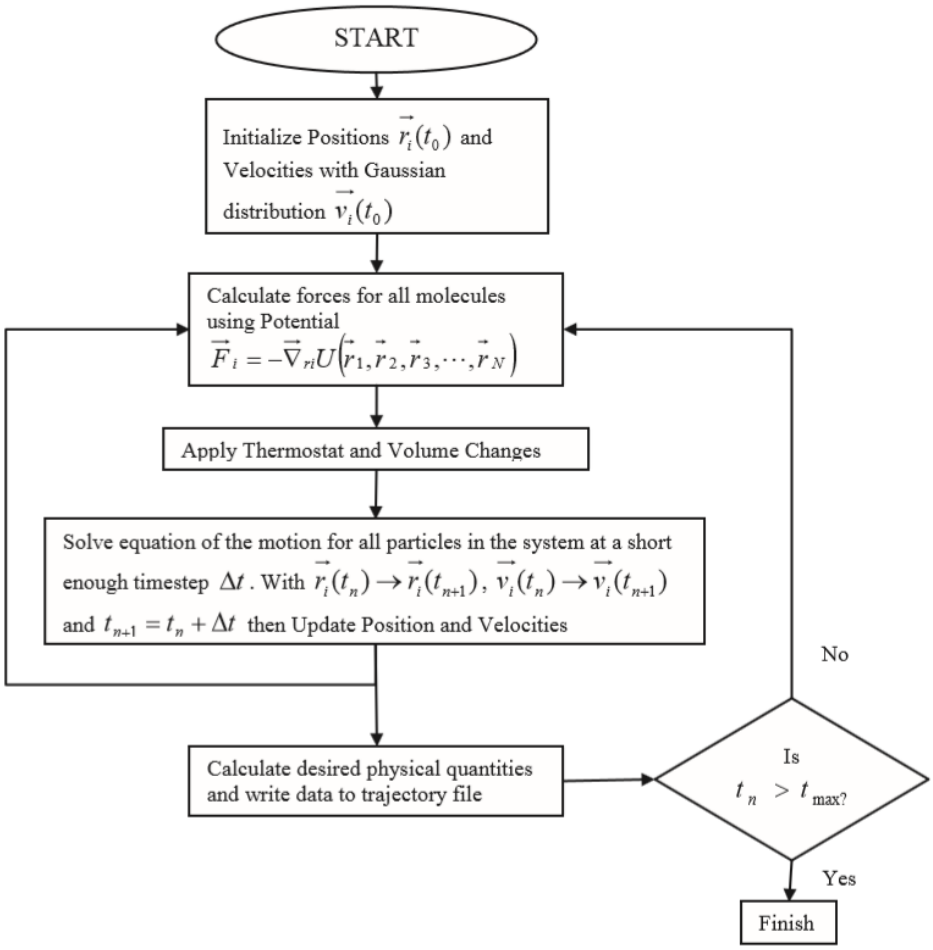

Figure 8: General algorithm of molecular dynamics simulations. Taken from [19]

2.1.1. Equations of motion

MD is a simulation technique for computing the equilibrium and transport properties of a classical many-body system. Given an initial set of positions and velocities of a system of N atoms, each atom is treated as a point mass, and the atomic motion is investigated based on Newton's equations. It consists in solving the Newton's equations of motion to calculate all the atoms' positions and velocities, and is written as:

$$\vec{F}_i = m_i \vec{a}_i = m_i \frac{d\vec{v}_i}{dt} = m_i \frac{d^2 \vec{r}_i}{dt^2}, \qquad \text{(Equation 1)}$$

where m_i, r_i , v_i and a_i are the mass, position, velocity and acceleration of atom i in a defined coordinate system, respectively. The force F_i acts on each atom i and modifies its position, velocity, and acceleration. The components of these force fields are calculated from the interaction potential or the potential energy U of each atom:

$$\vec{F}_i = -\overrightarrow{\nabla_{ri}} U(\vec{r}_1, \vec{r}_2, \vec{r}_3, \dots, \vec{r}_N) \quad \text{(Equation 2)}$$

The potential energy can be obtained using empirical potential energy expressions, semi-empirical methods, or *ab-initio* approaches. In our case, we chose to use a potential called embedded-atom method (EAM) Potential, well suited for metals, and based on fitting models to *ab-initio* density functional theory (DFT) calculations. A more detailed description will be given in the next section.

After the definition of initial conditions and interaction potential, Equations (1) and (2) are integrated. The state of each atom with its coordinates and velocity is updated numerically at each time step and then the corresponding trajectories of the particles in response to applied force fields are also updated. The calculations of the potential energy and force fields applied to the particles of the system require the bulk of the computing processing power.

2.1.2. Time integrator

A time integrator dictates the accuracy of trajectories at each time when the second-order differential equations of motion are solved. A time integrator, first introduced in 1960, known as the Verlet algorithm has shown reliable results. This algorithm is discussed here only for a single particle in one dimension to simplify the derived equations.

$$\tilde{x}(t + \Delta t) = \tilde{x}(t) + \tilde{v}(t)\Delta t + \frac{\tilde{a}(t)\Delta t^2}{2} + \frac{\tilde{b}(t)\Delta t^3}{6} + o(\Delta t^4) \quad \text{(Equation 3)}$$

$$\tilde{x}(t - \Delta t) = \tilde{x}(t) - \tilde{v}(t)\Delta t + \frac{\tilde{a}(t)\Delta t^2}{2} - \frac{\tilde{b}(t)\Delta t^3}{6} + o(\Delta t^4) \quad \text{(Equation 4)}$$

After adding Equation 3 and Equation 4 :

$$\tilde{x}(t + \Delta t) = 2\tilde{x}(t) - \tilde{x}(t - \Delta t) + \tilde{a}(t)\Delta t^2 + o(\Delta t^4) \quad \text{(Equation 5)}$$

The velocity is calculated from:

$$\tilde{v}(t) = \frac{\left(\tilde{x}(t+\Delta t) + \tilde{x}(t-\Delta t)\right) + o(\Delta t^3)}{2\Delta t} \quad \text{(Equation 6)}$$

2.1.3. Many-body interactions

As mentioned earlier, force fields are calculated from the potential energy of the system, and a realistic representation of elements with a crystalline structure requires counting the influence of close neighbors within the potential scheme. Metal atom interactions are particularly well described using the EAM. This method was first introduced by Baskes and Foiles (1986) [21], and the total-electron density in a metal is a linear superposition of contributions from the individual atoms. For each atom, the total electron density is a sum of three scalar functions: the embedding function, an electron cloud contribution function, and a pair-wise interaction. The embedding function corresponds to the electron density of the atom in question, the electron cloud contribution is a constant background density due to the electron density contributions of surrounding atoms, and the pair-wise interaction is function of the distance between two atoms and represents their electrostatic core-core pair repulsion. Assuming a metal system with N atoms, the total potential energy can be expressed as [22]:

$$E_{pot} = \sum_{i=1}^{N} E_i = \frac{1}{2}\sum_{i=1}^{N}\sum_{i,j,i\neq j}^{N} \emptyset_{ij}(r_{ij}) + \sum_{i=1}^{N} F_i(\rho_i) \qquad \text{(Equation 7)}$$

where E_i is the potential energy of atom i, Φ_{ij} (r_{ij}) is the pair-wise interaction of atoms i and j separated by a distance r_i, and F_i is the embedding energy term for the local electron density ρ_i at the position of atom i. Finally, the local electron density is a linear summation of the electron density contributions from all surroundings atoms j at the site of atom i. Each individual constribution is called $f_i(r_{ij})$:

$$\rho = j, j \neq 1N f_i(r_{ij}) \qquad \text{(Equation 8)}$$

2.2. LAMMPS

The large-scale atomic/molecular massively parallel simulator (LAMMPS) is an open source software supporting a molecular dynamics simulation package. It was developed by Sandia National Laboratories, USA, (http://lammps.sandia.gov/) [23] which also provides a manual of commands and rules to write an input script. Various types of systems can be simulated, e.g. atoms, polymers, biological molecules, metallic particles, granular and coarse grained systems and their transport properties can be observed in solid, liquid or gas states. Moreover, serial or parallel simulations can be run from a single script, which can considerably reduce the time requirement of certain simulations [24].

A considerable amount of pre and post processing tools are included in the LAMMPS package, giving the possibility to convert back and forth input or output files to the desired format. All these reasons explain its popularity in the simulation of NC deposition and relaxation of the system. The input script used in this work has been written using LAMMPS code and incorporates several of its features [25].

2.3. ATOMEYE

AtomEye is open source software [26] available for pre or post processing files from LAMMPS and for visualizing in 3D the trajectories of the observed atoms. It allows several features such as the creation of animations for detailed movements of particles in the system and a customization of the atoms' color based on the atom type, bond angle, kinetic energy, and more. These general features will prove useful in this work.

Chapter 3: Simulation of multiple clusters deposition on a substrate

3.1. Simulation set-up

MD simulations are carried out in a three dimensional space using LAMMPS. The LAMMPS code has enabled visualization of several clusters impacting on a substrate, and the different steps are summarized in the following block diagram schematic (Figure 9): first, the simulation starts with an equilibration at 300 K for 20 ps applied to the entire simulation box. Then each time period (set differently depending on the particle velocity studied), a cluster of atoms is released towards the substrate. The time period ranges from 5 ps for 0.022 eV/atom, 8 ps for 0.089 eV/atom and 20 ps for 0.358 eV/atom. During the entire simulation, a Nose-Hoover thermostat is continuously rescaling the substrate temperature to 300 K by modifying the velocities of the atoms. This feature allows the simulation to accurately represent the experiment, since in the experiment the NPs are deposited at room temperature in the LAMA technique. The process is repeated until the desired number of clusters is deposited. The maximum number of clusters deposited is equal to eight in our work. Finally, the trajectories of the atoms and the properties of interest are extracted into readable output files (text, image, or animation format).

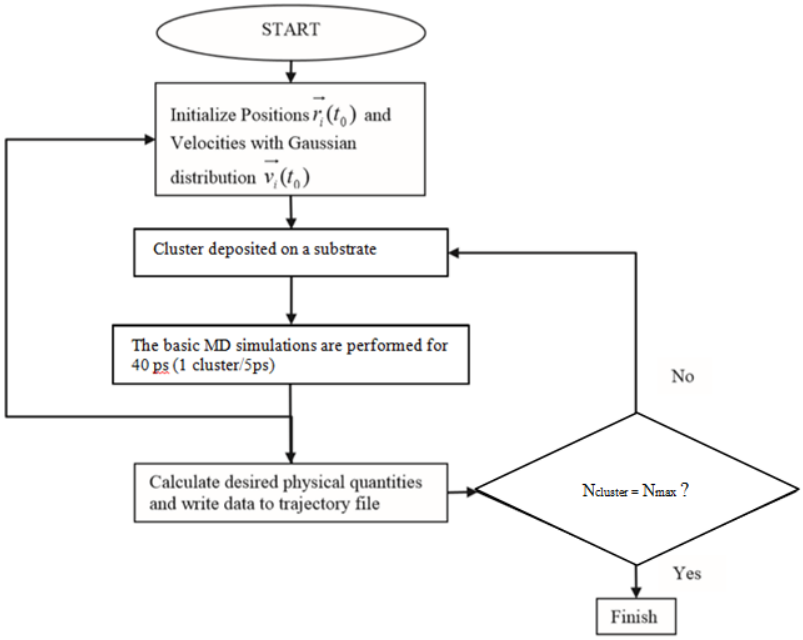

Figure 9: Block diagram of MD simulations modeling multiple cluster deposition on a substrate

A simulation box is created to set the boundaries of our simulations (Figure 10). The size of the simulation box has dimensions of 30×30×80 atomic unit cells and remains constant during the simulation run. Periodic boundary conditions are applied on all faces delimiting the simulation box to mimic physical characteristics within a bulk material and to allow relevant comparisons with experimental results.

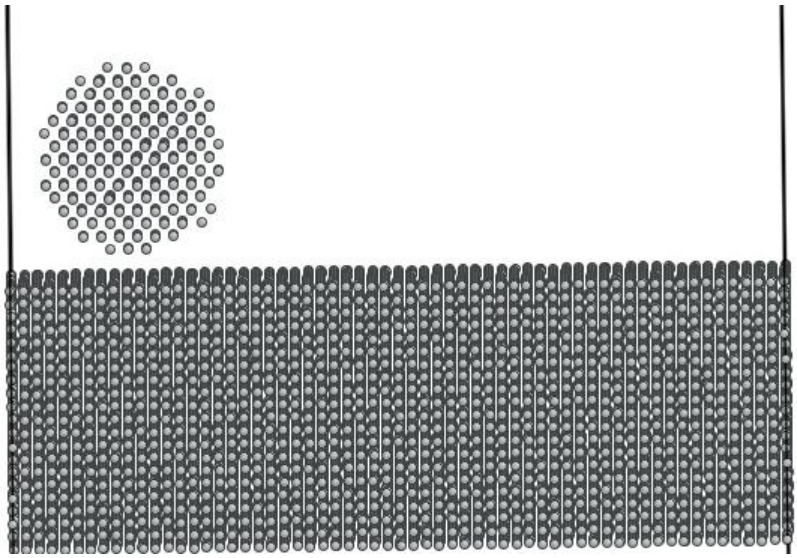

Figure 10: Simulation box containing a single NC and the substrate whose lattice structures are both periodic fcc unit cells. The NC and substrate in this case have different orientations.

Clusters are deposited with a normal incidence on a uniform 3D substrate. Each fcc unit cell (Figure 11) is periodically repeated in x y z directions to build the substrate crystal structure. The substrate dimensions have been set to 30×30×10 atomic unit cells for the 3 nm NC depositions (corresponding to 37,800 atoms) and 40×40×10 atomic unit cells for the 5 nm NC depositions (corresponding to 131,200 atoms). The substrate temperature is rescaled to 300 K each 100 fs for the highest impaction velocity (0.358 eV/atom) and each 1 ps for the other velocities. This leaves the dynamics of the substrate top layer free of constraints during the early stages of the cluster-substrate interaction and thus yields more realistic results. All the atomic positions and velocities of the substrate are adjusted according to Nose-Hoover dynamics, enabling them to act as a thermostat and hence to dissipate the perturbation after a cluster impact. In fact, right after a cluster is deposited, the substrate reaches a non-equilibrium state. The Nose-Hoover thermostat maintains the substrate temperature at 300 K by dissipating the excess energy

of the deposited cluster and its surroundings. The transport of heat within the substrate enables it to reach an equilibrium state again.

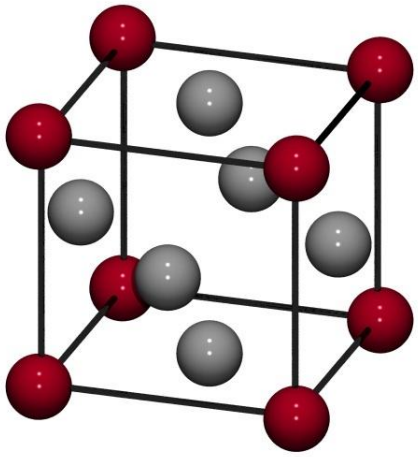

Figure 11: Face-centered cubic crystal structure unit cell - lattice unit a = 4.09 Angstroms for silver (Taken from http://johncarlosbaez.wordpress.com/2012/04/15/ice/)

Each cluster deposited is a sphere with a periodic fcc lattice of a fixed size set by defining its radius value. This corresponds to 2,000 atoms for 3 nm diameter NCs and 10,000 atoms for 5 nm diameter NCs. NCs are consecutively released at a random position in the x-y plane and high enough above the substrate to avoid the overlap with the growing film layer as the clusters are initialized. The cluster's lattice is oriented 45° in (x-y) with respect to the substrate lattice. Three NCs velocities were studied in this work: 200 m/s (0.022 eV/atom), 400 m/s (0.089 eV/atom) and 800 m/s (0.358 eV/atom). Impaction energies were varied within the range of 0.01 eV/atom to 0.5 eV/atom, which corresponds to a low energy impaction. Harbich *et al.* have shown that only epitaxial or non-epitaxial configurations were observed for these conditions [10].

The integration time step used was 1 fs and, as mentioned previously, clusters were released every 5 ps, 8 ps or 20 ps for the impact energies of 0.022 eV/atom, 0.089 eV/atom and 0.358 eV/atom.. The simulation runs for a total of 80 ps for the lowest impaction velocity (allowing 5 ps after the last impact for equilibration). It runs for 64 ps for the middle velocity (allowing 8 ps for final equilibration), and it runs for 220 ps for the highest impact velocity (allowing an extended final equilibration time of 80 ps from the last impaction). Our set-up gives

us very high deposition rates compared to the experimental values, varying from 5.65×10^{20} to 6.64×10^{21} NCs/s/cm^2 as opposed to 1.0×10^{10} - 1.0×10^{11} NPs/s/cm^2 in typical LAMA experiments [11]. Despite the high deposition rates in our simulations, we have observed that our settings still warrant a full relaxation of the system before the next cluster impact occurs for 3 nm diameter clusters. It is not true for 5 nm diameter clusters because of MD simulation limitations we will discuss later on. In fact, the time period separating two consecutive clusters disposition is chosen so that the substrate and the deposited cluster can completely be relaxed and the substrate temperature is stabilized at 300 K. Other simulation parameters discussed below were correlated to the typical experimental conditions of a supersonic aerosol jet deposition using the LAMA process.

3.2. INFLUENCE OF DEPOSITION PARAMETERS ON CLUSTER DEPOSITION

3.2.1. Cluster velocity

NCs were initialized with a normal velocity without assigning them an angular momentum as their angular rotation is not in our scope of study. Previous studies by Huang *et al.* [14] investigated how particles are accelerated in an aerosol jet. Since the impaction angle is very small, it is assumed that NP deposition is governed by the normal velocity and the influence of the impaction angle is neglected. The Ag NPs accelerated through a 250 micrometer orifice nozzle reach impaction velocities of 200 - 1200 m/s, depending on the composition of the aerosol gas (Ar or He). To be able to correlate our simulations with the experimental results, we will study three cases of cluster velocities: 200 m/s (0.022 eV/atom), 400 m/s (0.089 eV/atom) and 800 m/s (0.358 eV/atom). A significant advantage of MD simulations is that no specific calculations of molecular bonding energies, adsorption sites or crystallinity of the deposited layers need to be made to model a correct physical problem. Moreover, the range of energies covered in our simulations is well below the binding energy of Ag (equal to 4.8 eV, according to Figure 12), which should avoid more complex deposition behaviors than epitaxial and non-epitaxial mechanisms.

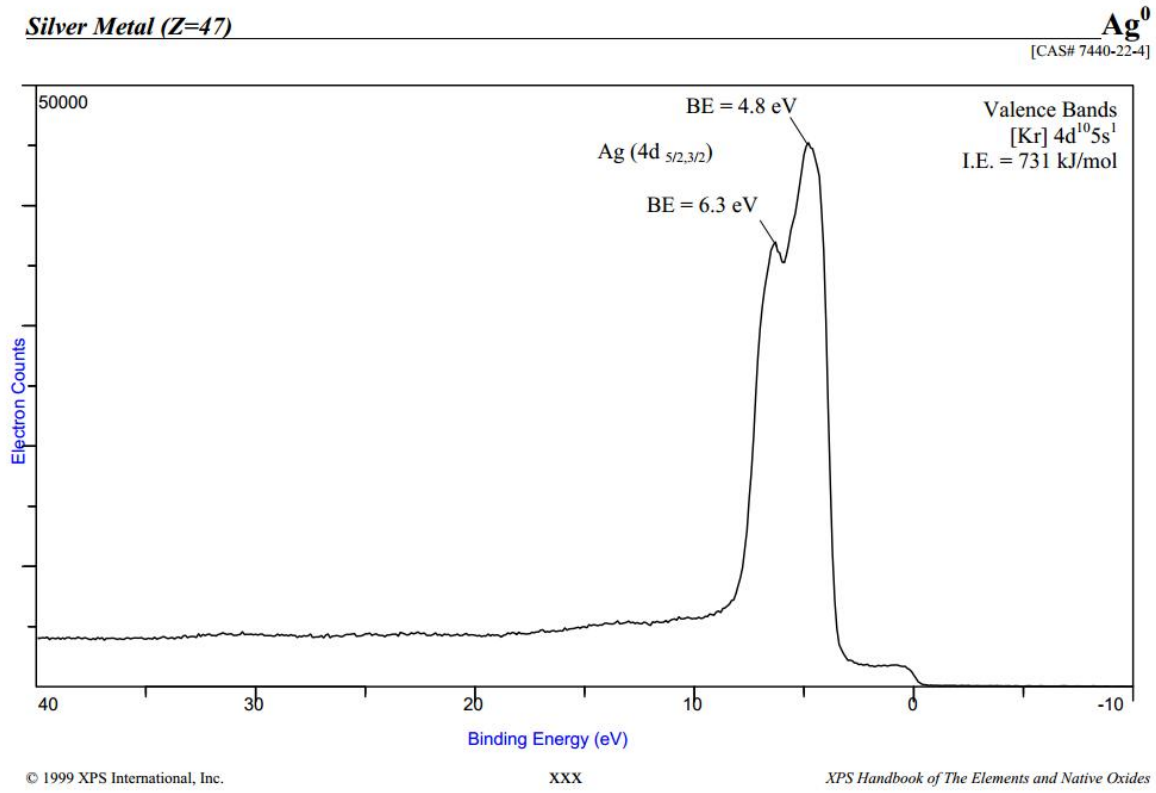

Figure 12: The atomic binding energy of Ag. Taken from [27]

3.2.2. Cluster size

The cluster size was given by the NC radius in our simulations and is determined by the number of atoms within the sphere. We studied two different cluster diameter cases: one of 3 nm corresponding approximately to 2,000 atoms and another of 5 nm corresponding to 10,000 atoms. Previous MD simulations by Haberland *et al.* [7] have studied the influence of the cluster size on the morphology of deposited thin films and have identified a cluster size limit to observe a complete epitaxial arrangement. Moreover, the complexity of MD simulations increases quickly with cluster size, and the program execution was either slowed down or crashed if we tried to solve calculations for tens of thousands of atoms for long times using a laptop computer.

The cluster size has been chosen to model typical LAMA deposition for silver. In fact, using the LAMA process, Gleason *et al.* [11] synthesized thin films by depositing Ag NPs of a few nanometers diameter (typically 5 nm) with a uniform size distribution and an aerosol feed rate of 1.0×10^{10} NPs/s/cm^3 (0.02 micrograms/cm^3). Typical NPs for this experiment are shown in

Figure 13. For the lowest feed rate that deposited single unagglomerated NPs, the 20th, 50th and 80th percentiles of the NP diameters illustrated in the figure are 3.5, 4.5, and 6.1 nm.

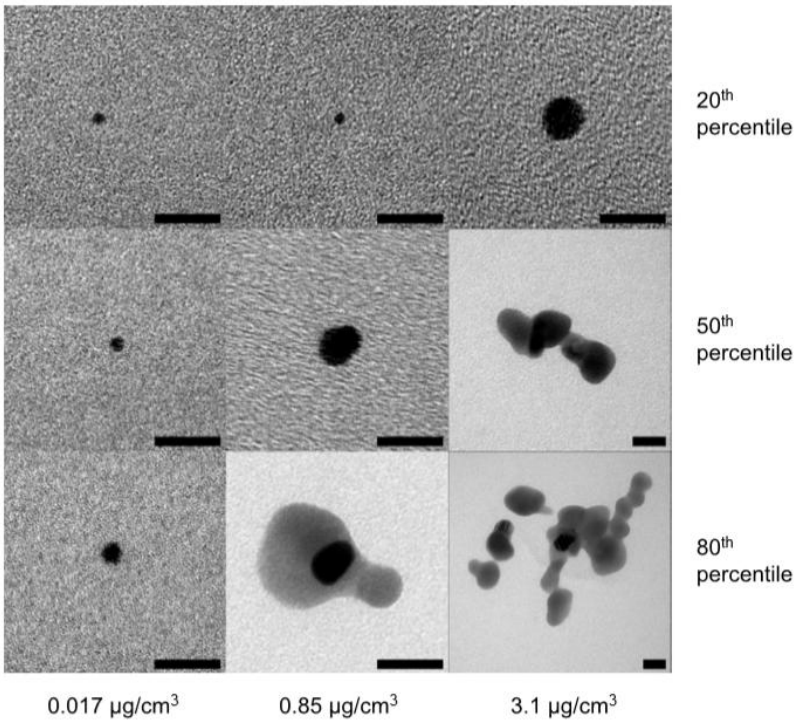

Figure 13: TEM micrographs of Ag NPs produced by LAMA, using He background gas. Each column illustrates, from top to bottom, the 20th, 50th and 80th percentile of the size distribution for one feed rate condition. Feed densities from left to right were 0.017. 0.85, and 3.1 µg/cm^3. Scale bars in each subframe represent 20 nm . Taken from ref [11].

3.2.3. Cluster initial position

The clusters were generated randomly in the x-y plane at approximately 5 to 10 lattice units (equivalent to 20-40 Angstroms) above the substrate in the z direction. For a simulation time of 80 ps, two clusters' impaction zones have a chance to overlap every 5 ps which leaves enough time to the impaction zone to return to equilibrium before another cluster interacts with the surface. It has been shown that the kinetic energy released between a deposited cluster and a smooth surface is very much larger than for the case of a cluster deposited over the distributed impaction zone prior to equilibrium being reached. This results in a smaller local temperature increase in the impaction zone, which reduces the chances of epitaxial alignment of the deposited clusters [28].

3.2.4. Deposition rate

In order to simulate a deposition comparable to a typical LAMA deposition, we created a substrate of 30×30 lattice units area, and the goal was to deposit films of thickness up to a few micrometers. However, these simulations would last up to hundreds of picoseconds, which is beyond the current limitation of our simulations. Thus, we focused on simulations that allow us only to observe the depositions that are a few nanometers thick.

The time interval between each released atom should be chosen to be greater than the energy relaxation time of the substrate after each collision, which lasts a few picoseconds and depends on the cluster initial velocity. The deposition rates simulated in our MD settings are large compared to experimental conditions. According to experimental results from Gleason *et al.*, NPs of 5 nm diameter with a narrow size distribution have been successfully deposited with a feed density of 0.02 micrograms/cm^3, which corresponds to 10^{10} NPs/s/cm^2 [11]. The deposition rates in MD simulations varied from 5.65×10^{20} to 6.64×10^{21} NCs/s/cm^2 if a cluster is released every 5 ps on a 30×30 lattice unit surface.

Modeling a deposition rate that reflects experimental observations appears to be quite challenging; however, we added a feature using a built-in command from LAMMPS to rescale the substrate temperature that helps relax the system faster. Thus, our results should be significant when compared to experiments as far as adherence, crystal structure, and morphology of the deposited films are concerned.

3.2.5. Substrate temperature

The substrate temperature is set to 300 K right before the clusters deposition starts and a Nose-Hoover thermostat is applied on the substrate to maintain a deposition at room temperature (300 K). The temperature evolution is reported during the simulation. It is a good way to identify if the deposited clusters are at equilibrium with the substrate. When a cluster hits the substrate, it increases the local temperature of the impaction zone and its surroundings. A displacement of the atoms lowers the substrate temperature by thermal conduction. While the system is cooling down, depending on the deposition conditions, we will observe the rearrangement of atoms once the final substrate temperature becomes stable.

3.3. BOUNDARY CONDITIONS

Periodic boundary conditions are applied on each dimension of the simulation box. This type of boundary replicates an infinite lattice in each axis direction and allows the simulation to mimic the bulk behavior within a decent computational time. The simulation box represents the central box, and there are exact copies repeated in such a way that if a particle leaves the central box; it will re-enter from the opposite face as shown in Figure 14.

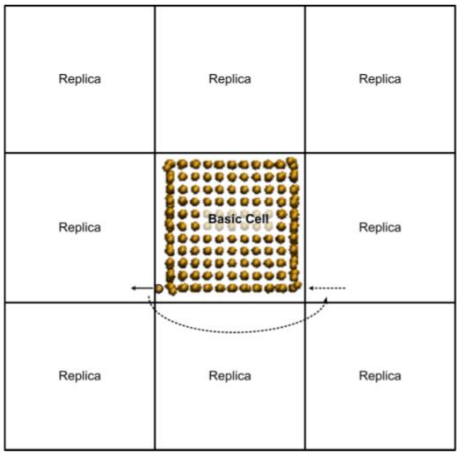

Figure 14: Representation of periodic boundary condition in x-y plane, where the middle cell is the simulation box surrounded by replicated cells. Atoms which leave the basic cell will re-enter from the opposite side

3.4. EQUILIBRATION

A system is said to be in equilibrium if its thermodynamic properties e.g. its temperature, pressure and volume do not vary when no external perturbation is applied on the system. It is very important to reach an equilibrium state to draw reliable, accurate and reproducible conclusions. Our simulation starts with an important equilibration step of 20 ps. Once all the clusters are deposited on the substrate, the film obtained is relaxed again for 5 ps to 40 ps before proceeding to its characterization.

3.5. THERMOSTAT

MD simulations were carried out in the NVT canonical ensemble, which means that moles (N), volume (V) and temperature (T) are conserved. Kinetic and potential energy exchanges occur and lead to fluctuations of the system temperature. However, a Nosé-Hoover

thermostat maintains the temperature at 300 K by adjusting the velocities of the atoms. T_{start} and T_{stop} both corresponds to 300 K since our system is relaxed at 300 K at the beginning and returns to 300 K at the end. A damping parameter of 100 time steps is chosen, which specifies how rapidly the temperature should be relaxed.

Chapter 4: Results and comparison of simulations with experiments

4.1. Context of the discussion

For low energy cluster beam deposition, different possible outcomes can be considered depending on simulation settings. They are detailed in this section. When a NC with an initial velocity hits the substrate, the cluster atoms within the layers directly in contact with the surface are abruptly decelerated. The cluster atoms within the upper layers are still moving towards the substrate and pile up after colliding with the front atoms. The pressure forces applied on the surface increase both potential and internal kinetic energies of the atoms within the cluster-surface interface. During this process, the cluster and its surroundings can achieve high values of temperature, density and pressure.

We will analyze the morphology and the structure of deposited films, particularly each cluster's final shape, the disorder depth, and the registration of the deposited material crystal lattice with the substrate. The aforementioned characteristics are key indicators to describe the cluster-surface interaction. We limited our scope to four types of cluster-surface interaction: plastic deformation, fragmentation, implantation and reflection of the incoming clusters. After the impact event, if the cluster sticks on the substrate and its shape is changed by the surface impact, plastic deformation may have occurred. This plastic deformation could be driven by dislocation motion, twin propagation, or amorphization. If the incoming cluster splits up into smaller aggregates, breaking atomic bonds within the cluster and reforming new atomic bonds between the cluster and the impact zone, a fragmentation occurred. Implantation describes an internal atomic mixing between deposited clusters and the substrate. The penetration depth of cluster atoms resulting from this implantation depends on its initial impact energy. Finally, reflection describes the case where cluster atoms bounce from the surface and there is no sticking on the substrate. These different possible outcomes after an impact event are summarized in Figure 15.

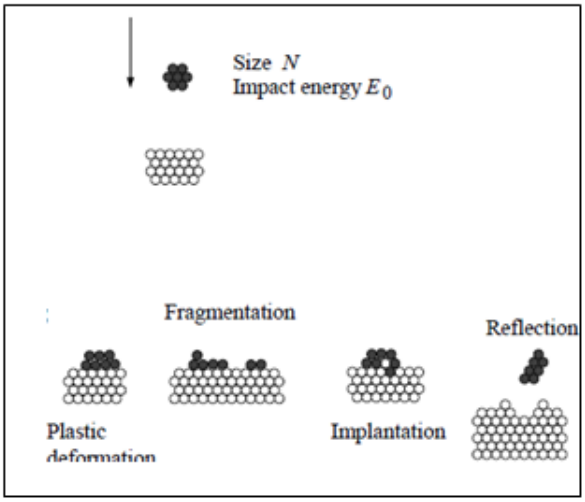

Figure 15: Possible outcomes of cluster-surface collision events

Crystal structure and adherence of the deposited films will be discussed to characterize the film morphology, and the parameters for our simulations. These characteristics will be quantified. As will be shown, altering the parameters previously described can change the film structure from amorphous to crystalline and can lead to the production of strongly adhering and smooth films. The quality of adherence of the deposited films can be attributed to the partial cluster implantation into the substrate after the impaction event. Defect-free epitaxial growth can be observed after recrystallization of the deposited layers at room temperature generally when local temperatures of cluster atoms and its surroundings become strongly elevated, and the cluster at impaction dissociates and spreads out into a uniform layer on the substrate.

4.1.1. Final shape

After a cluster is deposited on the surface with a given impaction energy, its particle deforms, and we need to wait sufficient time before we see its final state. Depending on the impaction energy (typically less than 1 eV/atom for low energy cluster bombardment), its final shape will be more or less flattened. We will measure the ratio of flattening, which indicates the degree of flattening of its final shape. To conduct these calculations, we will need to measure the cluster initial thickness right before it impacts the substrate and the cluster final thickness after impaction. The first measurement should be equal to the cluster diameter. The other

measurement should be done once its deformation is stabilized. After collecting this data, the ratio of flattening can be calculated using the following expression:

$$flattening\ ratio = 1 - \frac{final\ thickness}{initial\ thickness} \quad \text{(Equation 9)}$$

The flattening ratio is related to the level of homogeneity of the deposited film. For ratios of flattening that are low, it means that the deposited clusters form hilly structures on the substrate and form a collection of particulates that pile up and result in inhomogeneous layers. When the flattening ratios are high, the film morphology is smooth and relatively dense.

4.1.2. Disorder depth

Disorder depth represents the extent of displacement of atomic planes within the substrate after an impaction event. When a cluster hits the surface, it applies some compressive force to the atoms of the substrate. The intensity of compression can easily be tracked from our output files as it is proportional to the level of shading in the figures presented; darker shading implies more compression. Disorder depth is different from penetration depth. The latter involves atomic mixing between clusters and the substrate. It usually appears at the cluster-substrate interaction surface. The degree of sticking and adherence of the deposited film and the likelihood of epitaxial growth increases when the penetration depth is relatively high. By coloring the atoms of each cluster and the substrate differently, we are able to estimate the penetration depth and identify atomic mixing when it occurs.

4.1.3. Cluster-substrate lattice arrangement

The cluster-substrate lattice arrangement gives us information on the deposited film structure since it indicates how the cluster atomic planes are oriented relative to the substrate lattice. When the cluster hits the substrate, a transient disorder of its atoms and its surroundings is created and results in internal thermal energy transfer. The time needed for these atoms to come back to an equilibirum state is called relaxation time and can be tracked in the simulations by monitoring the local temperatures. Increased disorder will further elevate local temperatures and thus involve longer relaxation processes to come back to equlibrium. Figure 16 illustrates the case where the cluster-substrate lattice arrangement results in a recrystallization of the deposited film after impaction into an epitaxial film where there is alignment of the atomic planes within the substrate and the clusters.

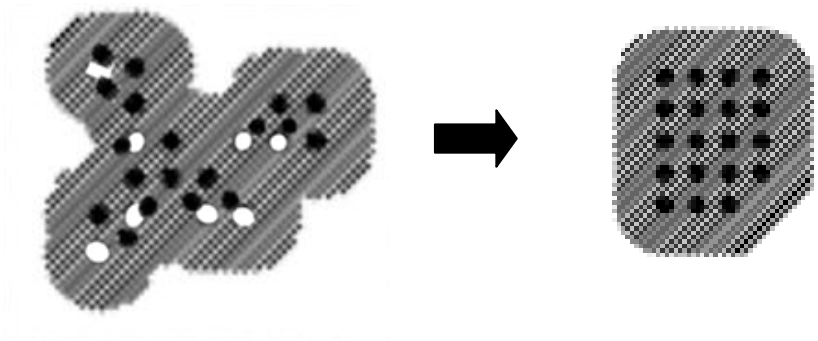

Figure 16: Recrystallization of disordered clusters leading to an epitaxial configuration

4.2. RESULTS

The results of our MD simulations are presented in this chapter according to two sets of parameters, the cluster impact energies taking the values of 0.022 eV/atom, 0.089 eV/atom, and 0.358 eV/atom and the cluster diameters of 3 nm or 5 nm. The output files of our MD simulations represent two different views depending the characteristics we are analyzing: a cut section of the (1 0 0) face at a depth of 0.5 (half way through the volume) and a plan view of the deposition surface from above (viewing the (0 0 1) face). The time step that appears on the figures is reset after the first thermalization of the substrate which lasts 20 ps. Figure 17 summarizes the different possible values of parameters in our MD simulations (values of cluster size and impact energy). As a reference, the boundary between epitaxial and non-epitaxial configurations drawn by Harbich *et al.* [10] for Au NCs deposition has been added.

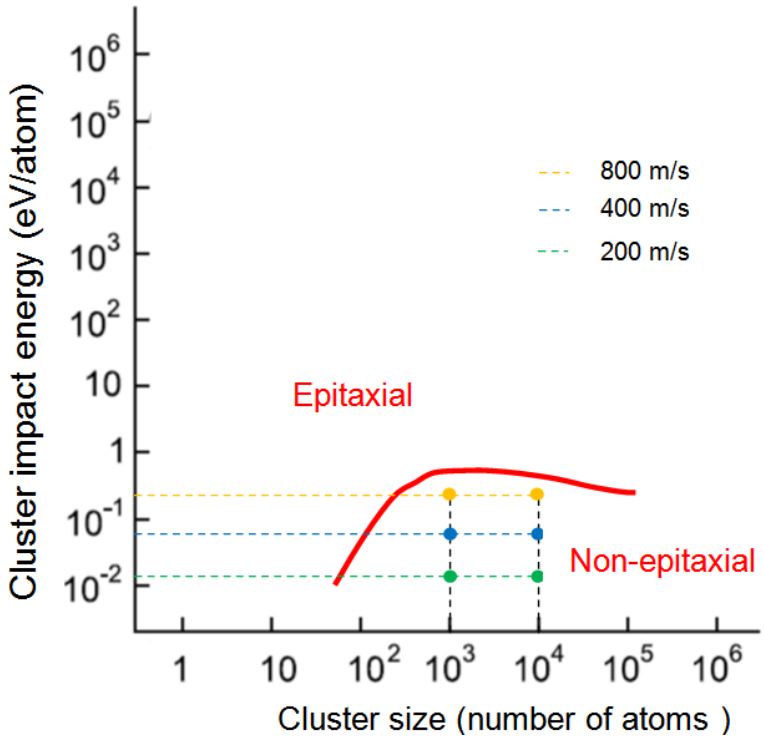

Figure 17: Values covered by our MD simulations according to cluster impact energy and size relatively to the epitaxy-non epitaxy configuration boundary of Au cluster deposition (taken from Harbich et al. [10])

The parameters of our MD simulations have been chosen so as to model comparable Ag NP depositions for LAMA process. Three main characteristics of the deposited films are analyzed from our MD simulations and compared to the experimental data if it is available: film density, crystal structure, and adherence.

Concerning the density of the deposited films, previous experimental studies have evaluated it quantitatively at room temperature by measuring quite precisely the mass density evolution while varying the aerosol feed rate. It has been shown that the density of the deposited films tends towards the bulk material density as the deposition energy is increased [13]. However, in our work, we only focus on the qualitative evaluation of density. Our scope is limited to observe whether MD simulations validate the experimental observations, For this purpose, the ratio of flattening, the mixing of atoms, and the possible presence of visible voids have been studied. They are good indicators to qualitatively analyze the evolution of the films density versus the cluster deposition energy.

For the analysis of film crystal structure, the position of the NC's atomic planes are compared to the substrate atomic planes. Epitaxy is assessed by comparing the orientations of the atomic planes in the substrate and deposited films. There is no quantitative data from the experiments to actually draw a precise epitaxy/non-epitaxy configuration boundary for Ag NPs deposition as has been drawn for Au NPs depositions by Harbich *et al.* [10], but it has been shown that an epitaxial growth is more likely to occur for the highest velocities within the range of 200-1200 m/s [13]. The boundary appearing on the diagram (Figure 17) comes from MD simulation results of Harbich *et al.* and is for the deposition of Au NCs, whereas we are simulating Ag NC deposition. We might first assume that this boundary holds for Ag NCs depositions and then validate or disprove this assumption when we analyze the obtained crystal structures.

We also want to draw conclusions about the ability of the deposited films to adhere to the substrate. It has been experimentally observed that Ag NPs bounce-off at the lowest velocities and have a higher sticking probability as the velocities increase [13]. The equivalent behavior for MD simulations would be to observe a complete NC bounce-off, not only small aggregates of atoms. This bounce-off behavior might not appear in the MD simulations since the substrate is cleaner and a more perfect crystal than it is for experimental depositions. When the cluster hits the top surface, the substrate is compressed and its atomic planes are displaced more or less deeply depending on the cluster velocities and size. The compression depth has been measured from the film top surface. A correlation between NC sticking and substrate disorder can be discussed if we assume that the binding energy is stronger when the atomic displacement is larger.

Our main challenge was to adapt simulation settings in such a way that it reflects experimental conditions and keeps a consistency between each case studied, whether we switch the size cluster from 3 nm to 5 nm, or vary the cluster energy. Moreover, we needed to ensure a complete or partial relaxation of NCs and substrate depending on the characteristic we were analyzing. Our goal is to be able to interpret our results from snapshots taken at comparable time steps between the two sets of velocities for 3 nm and 5 nm diameter NCs. However, we met some difficulties due mainly to the computing time limitations of MD simulations.

4.2.1. Qualitative analysis of density

- **The flattening ratio**

The flattening ratio is the ratio of the NC initial thickness before it impacts the substrate to its final thickness in the deposited.

To measure the flattening ratio, we do not need to achieve the complete relaxation of the clusters and the substrate as it is shown in Figure 18, because the height of the deformed cluster measured is almost the same before and after relaxation.

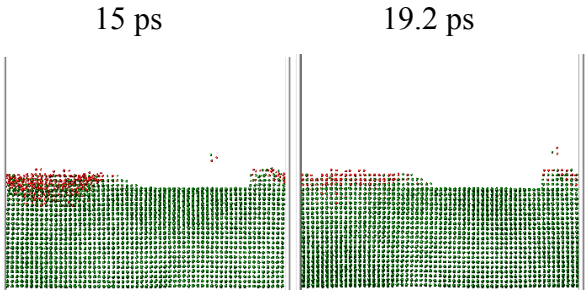

Figure 18: Comparison of the flattening ratios between a partial and a complete relaxation of a 3nm diameter cluster (shown in red) with an impaction energy of 0.358 eV/atom

Figure 19 shows snapshots taken after the first cluster deposition for each diameter at three different velocities. It is quite obvious from these pictures that NCs impacted at higher velocities tend to deform more on the substrate. We mentioned earlier that we do not need to wait until the complete relaxation of the system to measure the flattening ratio. This assumption simplifies the cases where NCs and substrate need a longer time to stabilize, and is particularly useful for the 5 nm diameter clusters, for which relaxation was hardly observable through our simulations because of the limited computing time scale (to be discussed later).

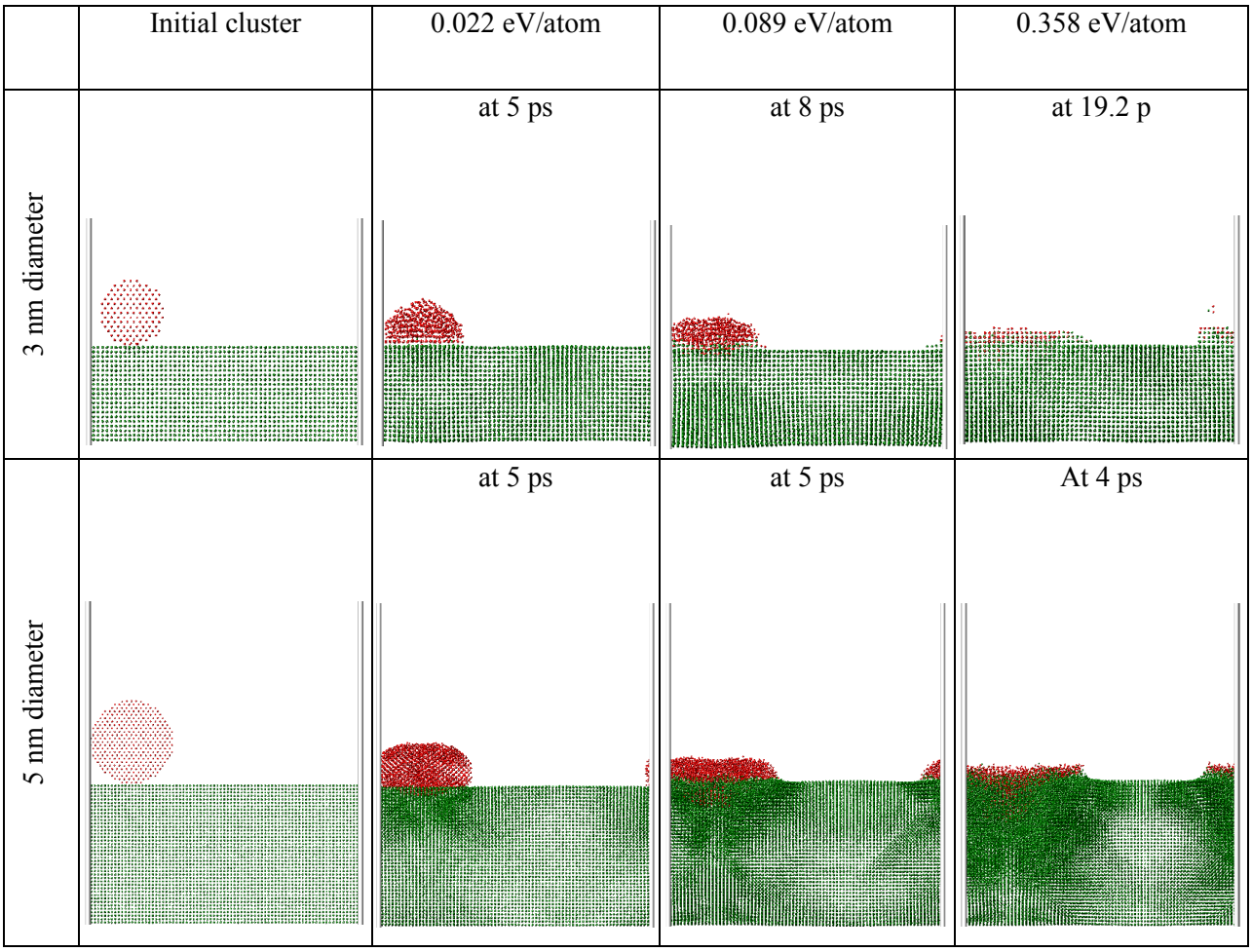

Figure 19: : Cross section view of the substrate after one cluster deposition comparing the initial cluster thickness with its thickness at 5 ps at different cluster impact energies (0.022 eV/atom, 0.089 eV/atom, and 0.358 eV/atom) for two different cluster diameters (3 nm and 5 nm)

Cluster initial thickness and its thickness once its deforms on the substrate have been measured from the snapshots taken in Figure 19. The obtained values allow us to calculate ratios of flattening for each case. All the calculations are summarized in Table III. As we predicted from Figure 19, the flattening ratio increases when the cluster impact energies increase, up to 85 % flattening for the highest energy case. The lowest energy case sets the lower flattening bound where the thickness of NC was reduced by half. It is also shown that the flattening of the recovered cluster does not depend on the cluster size because almost the same ratios of flattening are measured for a given energy whether the cluster diameter is 3 nm or 5 nm.

Table III:Ratio of cluster flattening at different impact energies 0.022 eV/atom, 0.089 eV/atom, and 0.358 eV/atom) for two different cluster diameters (3 nm and 5 nm)

		Ratio of flattening
3 nm diameter	0.022 eV/atom	0.5
	0.089 eV/atom	0.7
	0.358 eV/atom	0.85
5 nm diameter	0.022 eV/atom	0.46
	0.089 eV/atom	0.73
	0.358 eV/atom	0.85

- **Atomic mixing and flattening**

Figure 20 shows side views of the substrate after 8 Ag clusters have been deposited onto the substrate. Two cluster diameters (3 nm and 5 nm) and different cluster impact energies (0.022 eV/atom, 0.089 eV/atom, and 0.358 eV/atom) are shown. The results obtained are in agreement with what we observed previously after the first cluster deposition in terms of flattening. In fact, the shape of deposited clusters is more flattened as impact energies increase. The expansion of the incoming clusters reaches its maximum for 0.358 eV/atom Ag clusters, and leads to the formation of much more homogeneous layers compared to the 0.022 eV/atom and 0.089 eV/atom Ag clusters deposition. The mixing between atoms from different clusters increases as the impaction velocities are increased, which indicates that a stronger atomic binding is observable between clusters. Hence this could explain the reason why the deposited layers are more compact and dense as the velocities increase. These results are consistent for both the 3 nm or 5 nm cluster diameters.

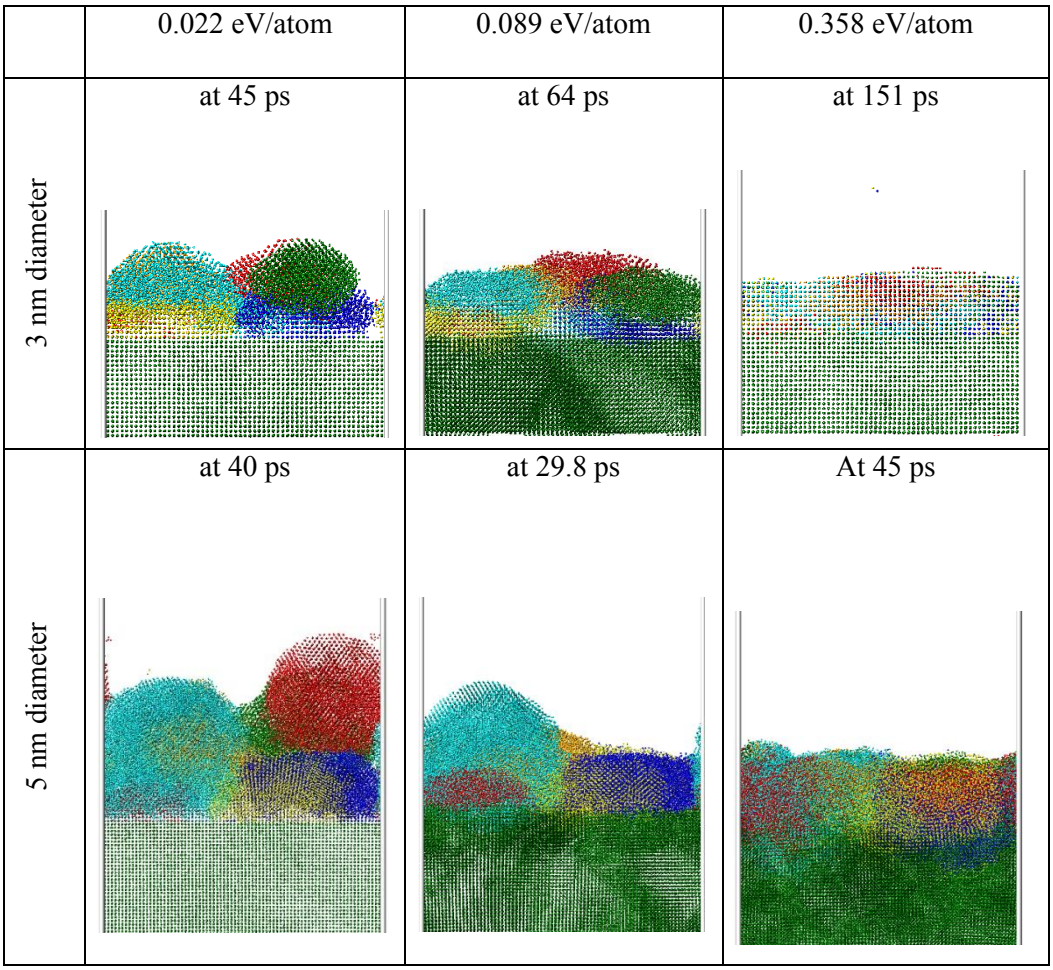

Figure 20: : Cross section views of the substrate after 8 Ag clusters deposition comparing the atom mixing and flattening of the deposited clusters at different cluster impact energies (0.022 eV/atom, 0.089 eV/atom, and 0.358 eV/atom) for two different cluster diameters (3 nm and 5 nm)

- **The visible voids**

We can clearly observe voids for the 0.022 eV/atom case that disappear for the 0.089 eV/atom and 0.358 eV/atom cases for both 3 nm and 5 nm cluster sizes in Figure 20. The 0.022 eV/atom Ag clusters deposition leads to the most porous layer as the deposited films is a collection of piled-up spheres that are flattened by 50%. We can expect a relatively high proportion of voids within the deposited layers in this case.

- **Comparison with the experimental density measurements**

MD simulations have shown an increase of both the flattening ratio and the mixing of atoms at higher velocities, and we can assume there are less voids at higher velocities. It agrees with the experimental density measurements obtained after supersonic laser jet deposition using

the LAMA process to deposit Ag NPs on a Si substrate. It has been shown that higher Ag NP velocities, e.g. in He background gas, up to 800 m/s, lead to denser thin films compared to films obtained using Ar background gas, for which the impaction velocities are 200-400 m/s [12].

A previous study of Ag NP deposition using the LAMA process for three different MP feed rates at 10 mg/hr, 20 mg/hr and 50 mg/hr, which correspond to a MP feed density of 0.85, 1.7 and 4.25 mg/cm^3, has shown that Ag NP agglomerates are larger and more numerous for higher MP feed rates. The increase of NP agglomerates fraction and size lead to more porous deposited films because agglomerates have a relatively low packing density [11]. We can compare our qualitative density results with the lowest MP feed rate because we did add NC agglomerates to our MD simulations.

Figure 21 presents previous as-deposited film density measurements using LAMA process deposition for three different MP feed rates of 10 mg/hr, 20 mg/hr and 50 mg/hr. As mentioned before, the most significant comparison between our simulations and experimental results concerns the deposition case at 10 mg/h MPs feed rate (equivalent to 0.02 g/cm^3). Hence, we will confine our discussion only to this case. We can see from Figure 21 that the measured film density is equal to 70% of the bulk density (10.49 g/cm^3). The deposited NPs in these experiments are mainly small spherical particles with a size distribution of 3-5 nm diameter. These density measurements of nanostructured silver films have been estimated experimentally by calculating the ratio of its mass over its volume. Its mass has been expressed by weighting the substrate before and after film deposition of dimensions of 4×4 mm^2 (with a precision scale of $\pm$ 0.00005 g) and its volume has been evaluated with a Zeta profilometer that acquired 3D surface profiles [13].

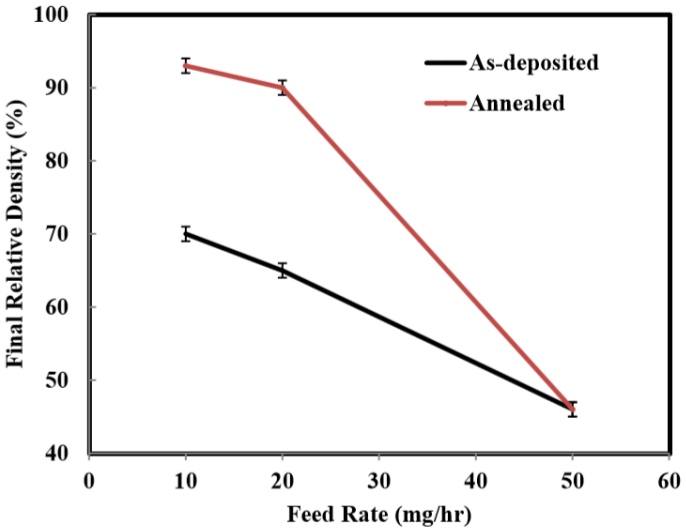

Figure 21 : Measurement of thin film densities after Ag NP deposition using the LAMA process for three different MP feed rates (0.85, 1.7 and 4.25 mg/cm3), taken from [13].

4.2.2. Crystal structure characterization

In this section, we focus on the observation of the atomic planes of both clusters and substrate. The evolution of their relative positions while the system is cooling after impaction events can give us quite a clear understanding of the atomic structure. For example, it can typically help us to know whether a complete or partial recrystallization occurs after NCs are deposited or if the deposited layers have grown in disorder or if there are visible defects and/or grains. Output files generated by LAMMPS are readable by AtomEye and this tool allows us to rotate the system in 3D and choose sections of interest to view if interesting crystallographic features are identified.

Figure 22 shows the evolution of the atomic lattice structure during the deposition of eight Ag clusters of 3 nm diameter at different cluster impact energies (0.022 eV/atom, 0.089 eV/atom, and 0.358 eV/atom) at the beginning of the simulation (1), after the first Ag cluster impaction (2), after eight Ag clusters have been deposited (3). After the first impaction, we can assume that the NCs are fully relaxed for all velocities, and we observe that there is some epitaxial growth visible at the bottom of the deposited cluster and that the upper part is quite disordered for both lower velocity cases. However, the highest velocity case shows perfect epitaxial growth after relaxation. For the case where 8 NC were impacted, we can assume again that the system is relaxed for all the velocity cases. The 0.022 eV/atom case shows some

epitaxial regrowth for the lower layers directly in contact with the substrate, but the atomic planes of the upper layers are clearly not aligned with those of the substrate. However, grain orientations may also not be entirely disordered. There is some evidence for the formation of polycrystal lie on top of an epitaxial layer. For the mid-velocity case, if we assume that NCs are relaxed, the epitaxial growth is even more prevalent in the lower layers directly in contact with the substrate than it was for the 0.022 eV/atom case. However, in this case, the film is clearly entirely disordered or amorphous in the top layers. Since silver is expected to crystallize and not remain amorphous at room temperature, it is reasonable to conclude that there has not been sufficient time for the particles to fully thermalized. To confirm this, the simulation would need to be run for longer times but this was not possible due to limitations of the available hardware. The highest velocity case shows again perfect epitaxial growth as the interface between the substrate and the deposited layer can no longer be distinguished from the substrate. If we assume that an non-epitaxial/epitaxial transition exists as the velocity increases, our observations for the simulations run for 3 nm diameters indicate that the transition might be between 0.089 eV/atom and 0.358 eV/atom. The transition clearly occurs at lower energies that that identified by Harbich *et al.* [10] for gold NCs shown in Figure 17. This is reasonable because Au has a higher melting temperature than Ag so that for the same deposition energy, the temperatures experienced by the particles upon impaction are a greater fraction of the homologous temperature for Ag. However, we would need to run more intermediate velocities to more precisely determine the precise transition energy.

(1) Initial state

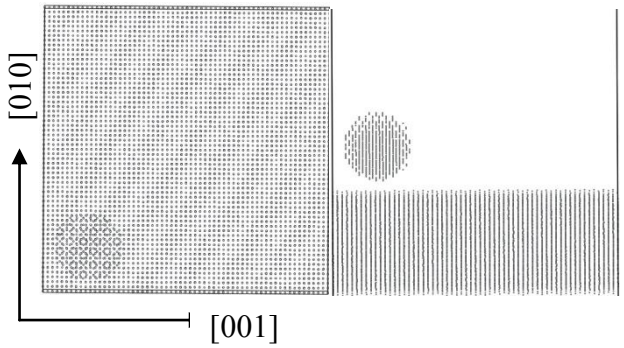

Figure 22: Evolution of the deposited film structure. Top view and cross section of the substrate at the beginning of the simulation (1), after the first Ag impacted cluster (2), after eight clusters deposited (3) for different cluster impact energies (0.022 eV, 0.089 eV/atom, and 0.358 eV/atom) (3 nm diameter cluster)

(2) First cluster deposition

	Top view (0 0 1)	Cross section (0.5 0 0)
0.022 eV/atom	at 5 ps 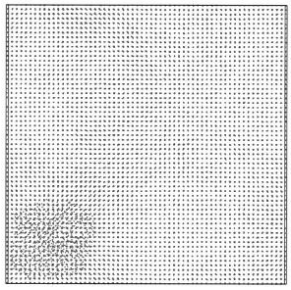	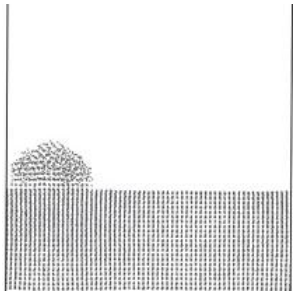
0.089 eV/atom	at 8 ps 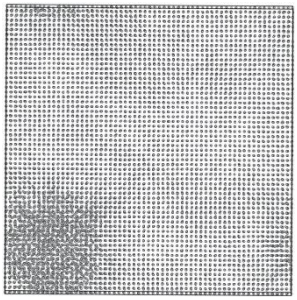	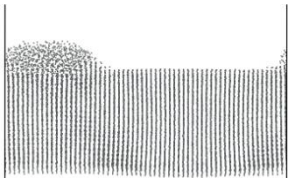
0.358 eV/atom	at 19.2 ps 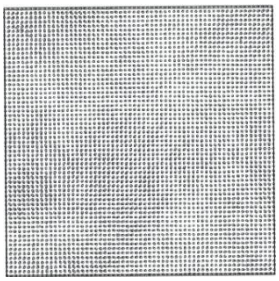	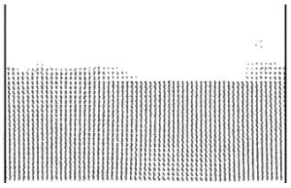

Figure 22, cont.

(3) After 8 clusters deposition

	Top view (0 0 1)	Cross section (0.5 0 0)
0.022 eV/atom	at 45 ps 	
0.358 eV/atom	at 64 ps 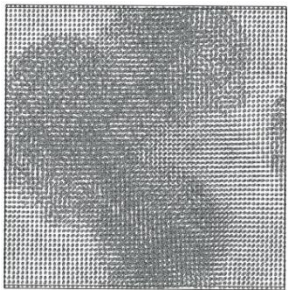	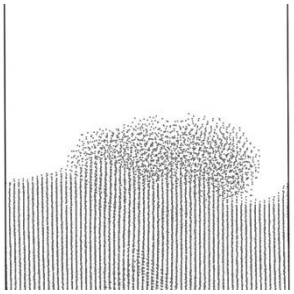
0.805 eV/atom	at 200 ps 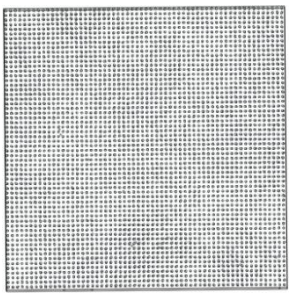	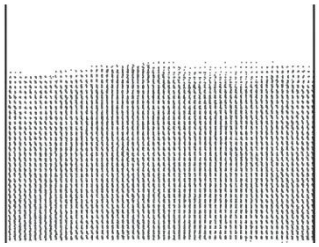

Figure 22, cont.

Figure 23 shows the evolution of the atomic lattice structure during the deposition of a single Ag cluster of 5 nm diameter at different cluster impact energies (0.022 eV/atom, 0.089 eV/atom, and 0.358 eV/atom) at the beginning of the simulation (1) and after the first Ag cluster impaction (2). For this cluster size, computing times are longer, and this limited our ability to

observe full relaxation of the system. For this reason, we have not been able to identify snapshots where the system was fully relaxed, even for the single cluster deposition case and for any velocity. We cannot draw conclusions concerning the crystal structure from only a partially relaxed system. This difficulty will be discussed in more detail later as one of the limitation in our MD simulations.

(1) Initial state

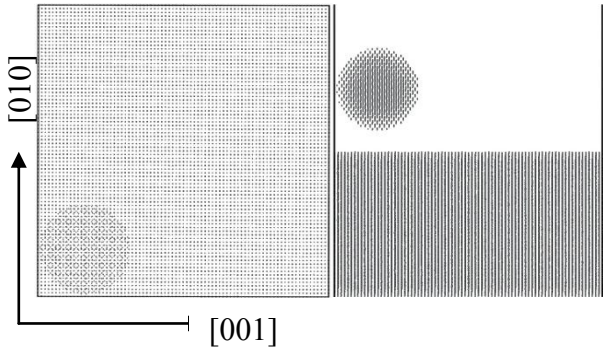

(2) After one cluster deposition

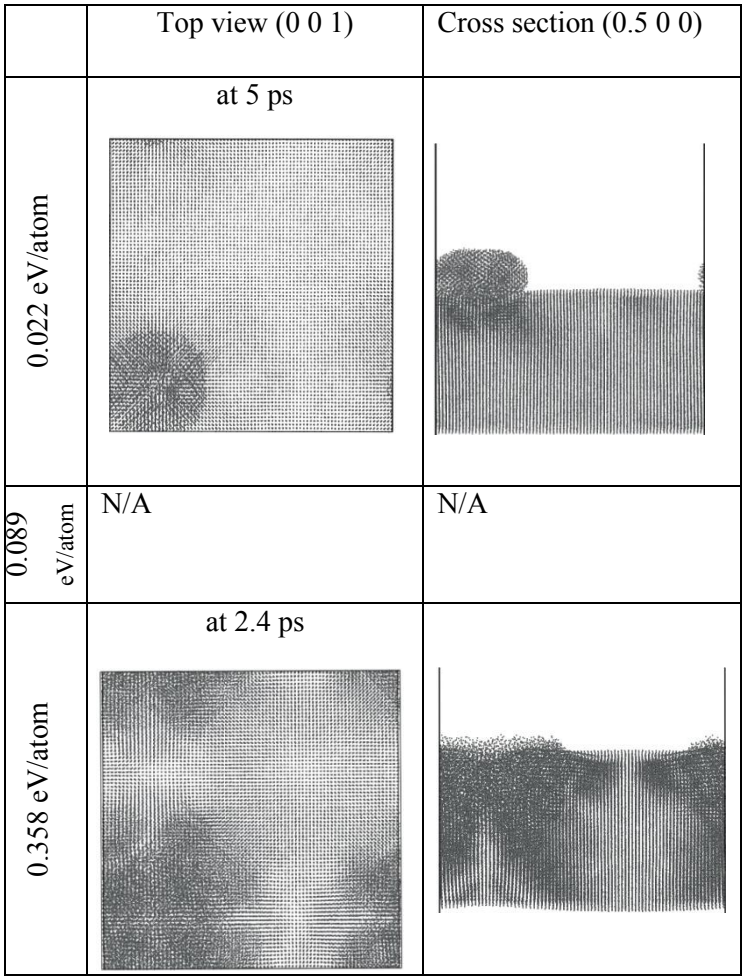

Figure 23 : Top view and cross section of the substrate at the beginning of the simulation (1), after the first Ag impacted cluster (2) for different cluster impact energies (0.022 eV/atom, 0.089 eV/atom, and 0.358 eV/atom) (5 nm diameter cluster)

4.2.3. Adherence on the substrate

Once a cluster reaches the substrate, its kinetic energy is transformed into potential energy, resulting in a compression of the atoms within the substrate. We observe a displacement of the atoms substrate along specific lattice directions. Figure 24 shows transient cases in the time interval 6.4 - 8 ps captured after deposition of 2 clusters for 3 nm and 5 nm diameter particles at different impact energies (0.022 eV/atom, 0.089 eV/atom, and 0.358 eV/atom).. Clearly the degree of compression (darkness) is proportional to both deposition energy and NC size. It raises a possible correlation between the disorder depth and the adherence on the substrate. In fact, for higher velocities, the disorder propagates deeper within the substrate, which indicates that the substrate is more energetically stimulated. Some mixing of atoms is even visible at the top surface of the substrate for the 0.358 eV/atom case. Deposition under higher cluster velocities involves inelastic processes, which increase the atomic binding energies between atoms from clusters and substrate, and thus could be correlated to the increase of deposited film adherence.

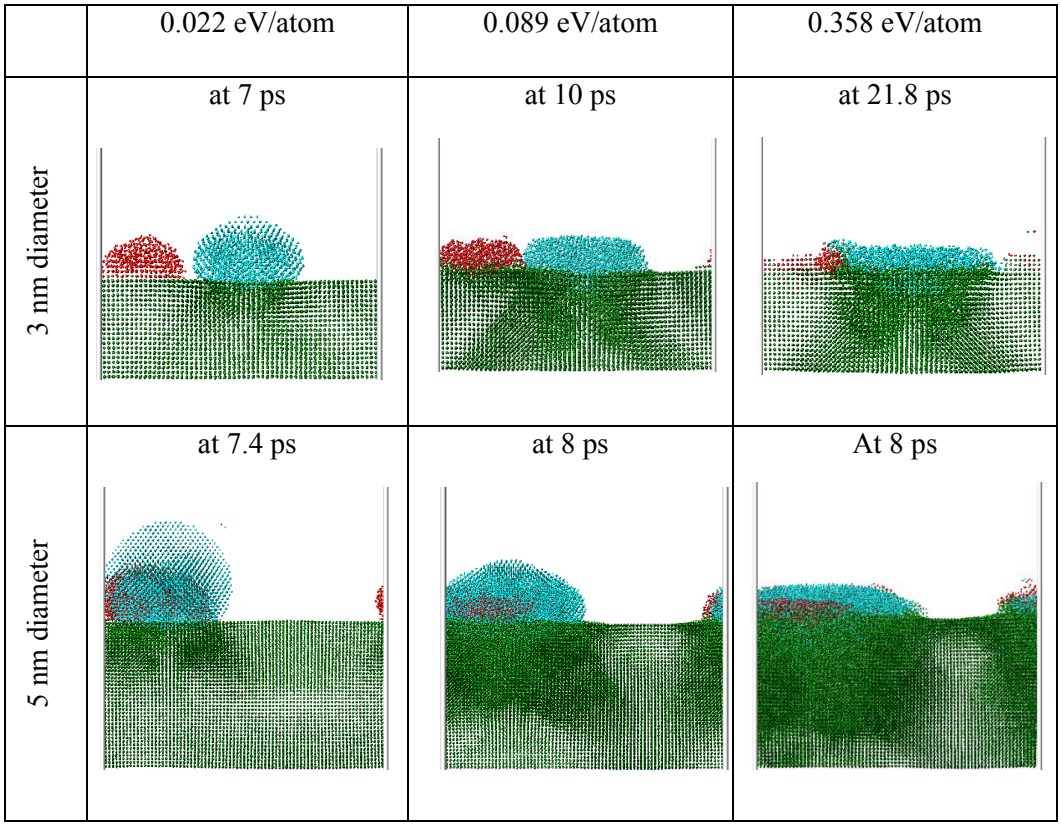

Figure 24 : Disorder depth after depositing 2 Ag clusters on the substrate (3 and 5 nm diameter) for different cluster impact energies (0.022 eV/atom, 0.089 eV/atom, and 0.358 eV/atom)

Previous experiments have studied the deposition of Ag nanostructured lines written at two different temperatures (25°C and 75°C) on bare Si/SiO_2 substrates at a feed rate of 10 mg/hr, 20 passes, and substrate translation speed of 0.635 mm/s. It is experimentally shown that higher impaction velocities and increased substrate temperatures increases adhesion as seen in Figure 25 [13]. For MD simulations, we hypothesize that we can correlate sticking with mixing without having to simulate NC deposition at higher temperature since cluster impaction kinetic velocity is ultimately converted to higher temperatures in the impacting particles and substrate. Thus, the experiments show that both increased substrate temperature and increased kinetic energy promote particle sticking.

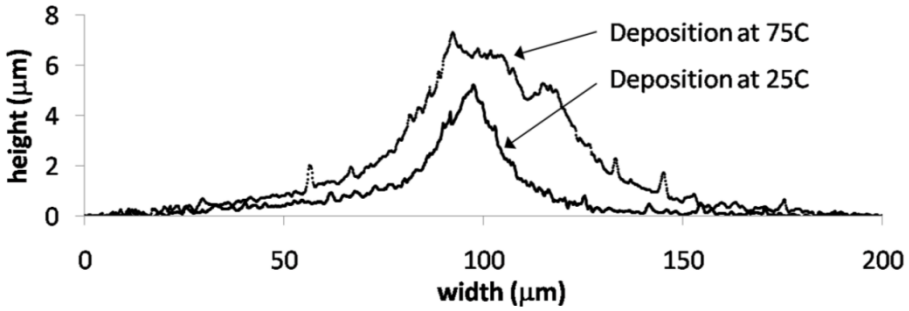

Figure 25: : Cross section of Ag lines written using LAMA deposition technique at two different substrate temperatures (25°C and 75°C) on bare Si/SiO2 substrates at a feed rate of 10 mg/hr, 20 passes, and substrate translation speed of 0.635 mm/s. Taken from [13]

Ag NPs have been observed to bounce off the substrate for the lowest MP impaction speeds according to previous experiments [13]. However, this phenomenon has not been observed with our MD simulations at the lowest impaction velocities. One possible explanation could be that the top surface of the substrate is actually cleaner and smoother in our computational model than it is the case for experimental conditions.

4.3. MD SIMULATION LIMITATIONS

4.3.1. Cluster and substrate relaxation time

We need to fully relax the substrate between each cluster deposition. This relaxation time is dependent on the cluster size and the cluster velocity. It is longer as the cluster size and velocity increase. It can vary from 5 ps for 3 nm clusters at 200 m/s to 20 ps for 3 nm clusters at

800 m/s. The relaxation times of the impacted cluster and the substrate have been measured in order to estimate the time needed between each impaction and for the thermalization step at the end of the deposition. As shown in Figure 26, we simulated the impaction of 8 clusters of 3 nm diameter with an impaction energy equal to 0.358 eV/atom (corresponding to the highest velocity 800 m/s). According to Table IV, we see that the relaxation time of the substrate averages around 10 ps, but can be as high as 13.6 ps. We observe that it takes more time for the clusters than for the substrate to relax once they hit the substrate. A cluster needs approximately 20 ps to deform completely on the substrate and achieve a stable configuration. The maximum time needed for a cluster to relax is after all 8 clusters have been deposited and lasts 27.8 ps. This corresponds to the thermalization step. This suggests that in order to make significant observations of the morphology of the film, we need to let the whole system return to its equilibrium state for 30 ps after the last impaction.

These observations have significant consequences for the time scale of our simulations. We have shown that we need to separate each cluster deposition by 20 ps and thermalize the whole system for approximately 40 ps after the last NC deposition. This represents a very long run in the MD simulation context, especially for NCs of 5 nm. For these reasons, we chose to simulate the deposition of only 3 nm clusters with full relaxation, and restrict the simulation of NCs of 5 nm diameter to a partial relaxation. We saw that the conclusions regarding the final shape of the clusters are not be affected because we do not need to be fully relaxed to get an estimation of the final NC height. However, it will affect the conclusions drawn for the structure of the deposited layers which cannot be properly interpreted from these simulations.

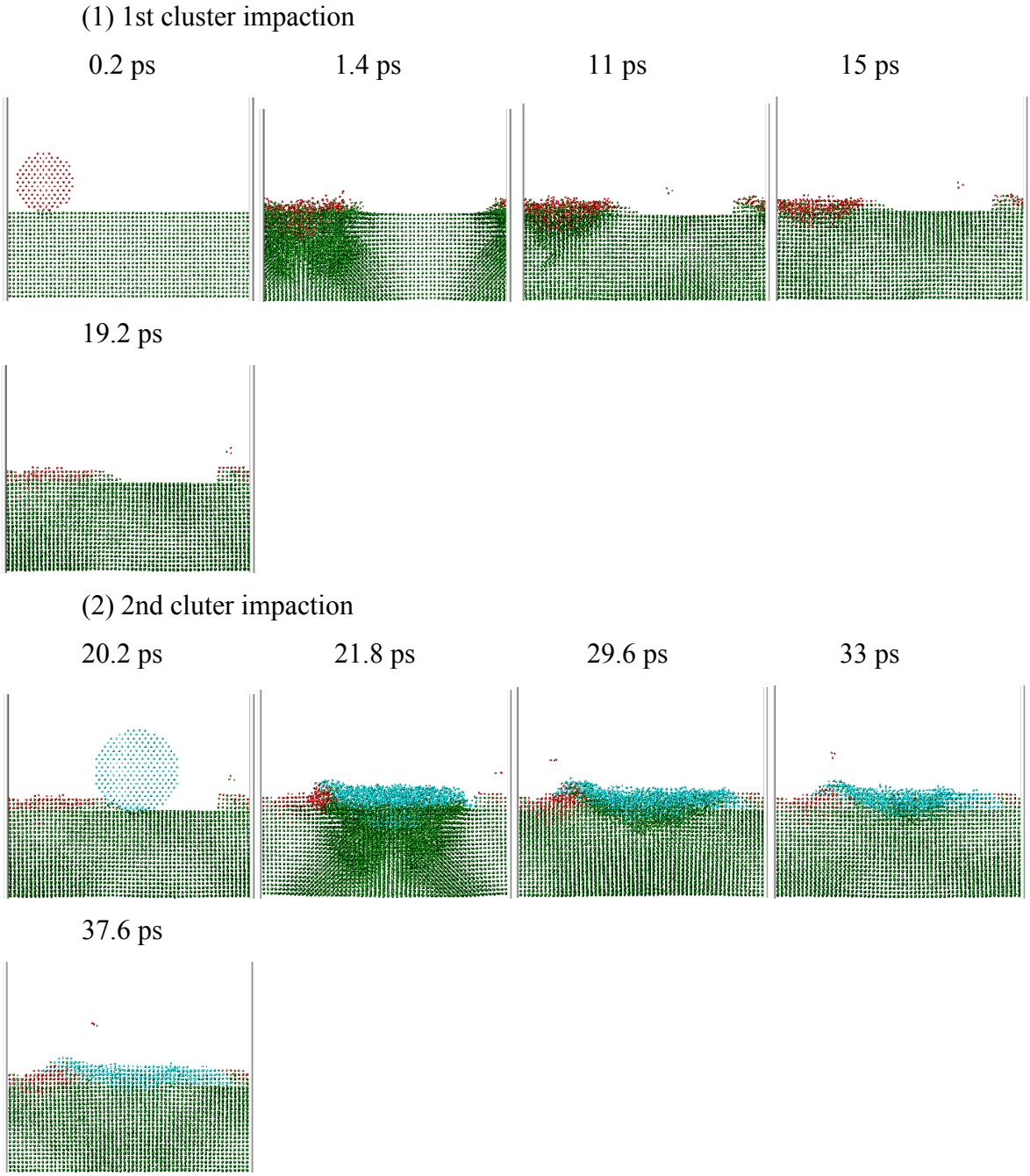

Figure 26: Evolution of the clusters and substrate relaxation versus time for a deposition of 8 clusters of 3 nm diameter given an impaction energy of 0.358 eV/atom for (1) 1st cluster impaction, (2) 2nd cluster impaction, (3) 4th cluster impaction, (4) 8th cluster impaction, (5) after 40 ps of thermalization

(3) 4th cluster impaction

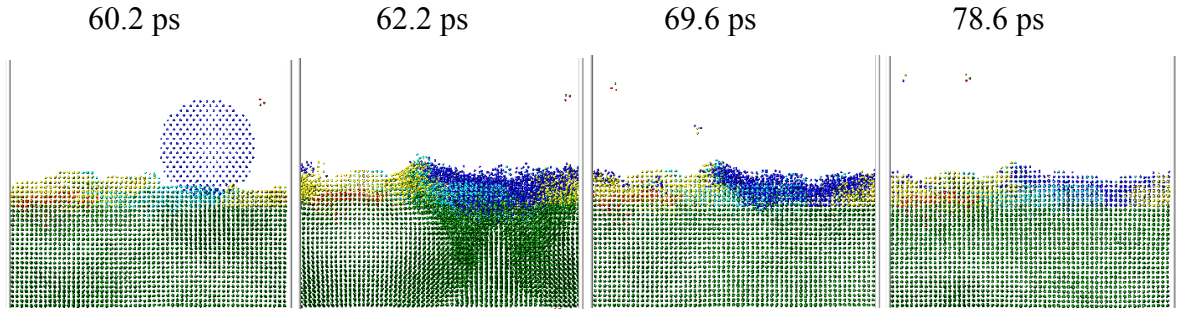

(4) 8th cluster impaction

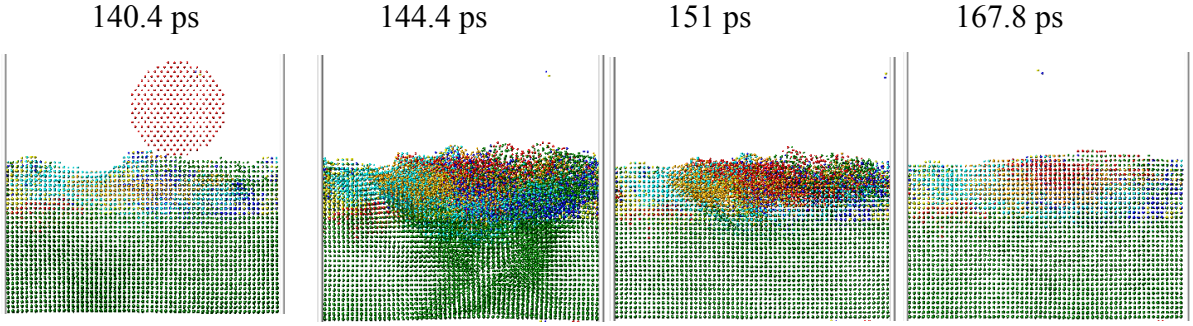

(5) after 40 ps of thermalization

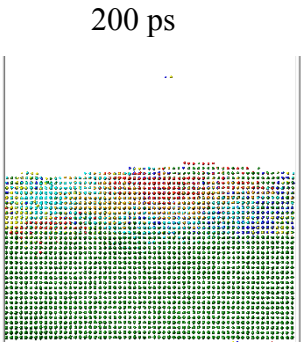

Figure 26, cont.

Table IV reports the relaxation times measured in picoseconds for the substrate and the deposited clusters for the deposition of Ag NCs at 0.358 eV/atom impact energy. We consider that the substrate and the cluster are relaxed once the darker regions fade (atoms return to their equilibrium lattice positions). For the cluster time relaxation measurement, we subtract the time step when the darkest region becomes bright from the time step right before the cluster impacts the substrate. For the substrate time relaxation measurement, we subtract the time step when the darkest region becomes bright from the time step when the disorder displacement is the deepest within the substrate.

Table IV: Relaxation times for the substrate and the deposited clusters for the simulation of eight clusters deposition

	Relaxation time - substrate (ps)	Relaxation time - cluster (ps)
1st cluster	13.6	19
2nd cluster	11.2	17.4
4th cluster	7.4	18.4
8th cluster	6.6	27.4

4.3.2. Time interval to rescale substrate temperature

Our aim is to simulate NC deposition at room temperature. To keep the substrate at a fixed temperature, we enforced a substrate temperature rescale after a given time interval. The substrate temperature needs to be rescaled more often if the substrate is more compressed, which is the case for the largest and fastest NCs. For 3 nm clusters at 200m/s, we needed to rescale the substrate temperature each ps as opposed to each 100 fs for 3 nm clusters at 800m/s. For 5 nm clusters at 200 m/s, it was set to each 500 ps. This feature also allows relaxing the system within shorter computational times. Figure 27 presents the evolution of the substrate temperature (K) versus time step in picoseconds for the deposition of 2 Ag NCs spaced by 20 ps, for 3 nm particles, at an impact energy of 0.358 eV/ atom. The temperature was rescaled every 100 fs to 300 K. We can clearly observe that the substrate temperature is fixed at 300 K during the simulation, except at the initialization of the simulation and at each impact event. We have previously stated that a cluster impact event will immediately raise the localized regions (?) of the substrate to very high temperature, up to 3000 K, according our results. However we can note that the excess energy is rapidly dissipated and the substrate temperature returns to its original temperature within less than 1 ps.

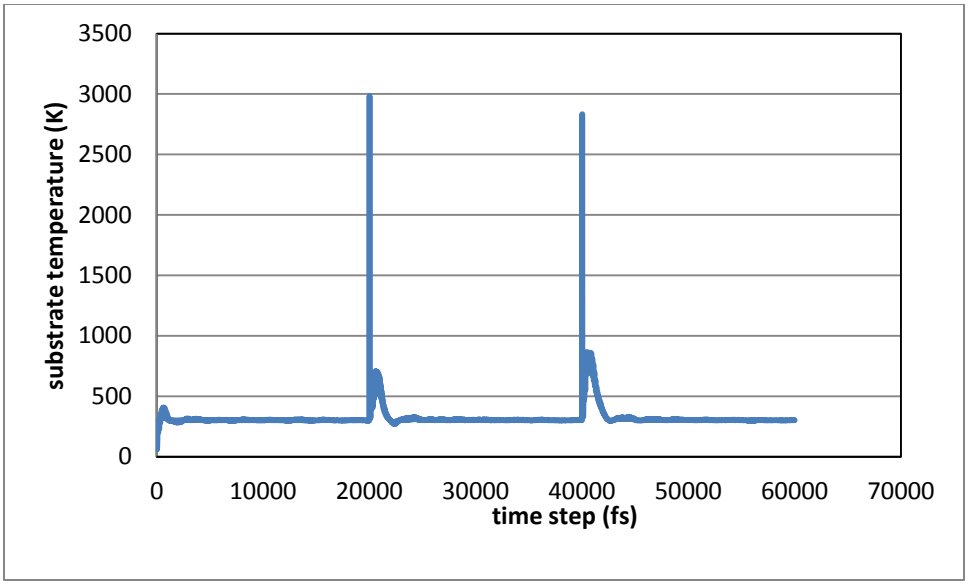

Figure 27 : Evolution of the substrate temperature (K) with the time step in femtoseconds for the deposition of 2 Ag NCs spaced by 20 ps, of 3 nm diameter, at an impaction energy of 0.358 eV/ atom

4.3.3. Simulation running time

Our MD simulations are subject to long run times, up to hundreds of picoseconds, which can take more than a day in real time to run on a single laptop computer. It is strongly dependant on the following settings: relaxation time, time interval to rescale substrate temperature, total number of atoms created, and impaction velocity. As these parameters increase, it slows down the simulations considerably and can lead to unreasonable computational times. It can also result in the simulation simply freezing if the memory needed exceeds that available on the computer. Simulations have crashed for the longest computing times and thus limited the results for simulation of 5 nm cluster deposition.

Conclusions

The density, structure, and the adherence of deposited NCs have been evaluated qualitatively in the scope of this work. The aim for our MD simulations was to model a specific deposition technique for Ag nanoclusters on a substrate called LAMA deposition. Variabiales for these simulations were the cluster size, the cluster impact energy, the deposition rate, and the substrate temperature. They were adjusted such that they reflected as closely as possible the actual experimental conditions. We wanted to be able to compare our MD simulation results with experimental results from the literature. The results obtained from experiments concerning the adherence, the crystal structure, and the density of the deposited films were compared to our computational results and seemed to validate our modeling when the experimental data was available.

It has been observed that low-energy cluster deposition should be an effective means for the deposition of very smooth and adherent epitaxial silver films, especially when the cluster impact energies are in the range 0.3-0.5 eV/atom (below the silver binding energy) for a cluster diameter in the range of 3-5 nm at room temperature. For the highest impact energy used in the simulations (0.36 eV/atom) and 3 nm NCs deposition, the relaxation time necessary to observe epitaxial growth of deposited films was a 20 ps.

For each case studied, we characterized the final film morphology, the film density, and the atomic planes direction of the incoming clusters. We also measured the disorder depth of the compression applied by the clusters on the substrate following impact events. We have been able to observe uniformly deformed layers in which the NCs show up to 85% flattening from their initial thickness for a cluster impact energy of 0.36 eV/atom. The film density also tends towards the silver bulk density for this range of energies. We also have observed the film properties were almost independent of the cluster size in the range of 3-5 nm diameters since we have drawn the same conclusions for both of these cases. Finally, epitaxial growth can been correlated to the level of thermal agitation that occurs within the substrate after the cluster impact event. It has been shown that increasing the deposition energy leads to a deeper propagation of atomic disorder within the substrate, and hence provides the thermal energy necessary to observe a recrystallization of the deposited layers.

Suggestions for future work

Of interest for future work would be to quantitatively measure a number of these properties using LAMMPS. One could implement a function that would count the number of atoms within a region. Given a molecular mass of Ag equal to 107.9 g/mol, we could convert the counted number of Ag atoms per volume to an atomic mass per volume, which corresponds to the mass density of the film. To test if the built-in commands from LAMMPS are actually performing correct calculations, we should start testing by computing the substrate density before the beginning of the NCs deposition. If it is correctly programmed, it should return the Ag bulk density equal to 10.49 g/cm^3.

Appendices

APPENDIX 1: INPUT SCRIPT FOR 5 NM CLUSTER DEPOSITION

The LAMMPS code used to simulate the deposition of 5 nm NCs is detailed below. The substrate is of dimension 40×40×20 lattice units. The deposition rate is fixed by releasing a new NC each 5 ps. The NC velocity is fixed to 800 m/s here. The first thermalization lasts 20 ps, the last one 5 ps. A log file reporting the simulation settings is generated and two different outputs are created, either a .jpg format or .cfg format.

```
# ------------------------ INITIALIZATION ----------------------------
units             metal
dimension         3
boundary          p         p         p
atom_style        atomic
variable latparam equal 4.09
# ----------------------- ATOM DEFINITION ----------------------------
lattice           fcc ${latparam}
region            box block 0 40 0 40 -40 55
create_box        9 box
region            substrate block 0 40 0 40 0 20
lattice  fcc ${latparam} orient x 1 0 0 orient y 0 1 0 orient z 0 0 1
create_atoms   1 region substrate
group substrate region substrate
# ------------------------ FORCE FIELDS ------------------------------
pair_style        eam/alloy
pair_coeff        * * Ag.eam.fs Ag Ag Ag Ag Ag Ag Ag Ag Ag
# -------------------------- SETTINGS --------------------------------
compute temp_substrate all temp/region substrate
# ----------------------- THERMALIZATION -----------------------------
reset_timestep 0
timestep 0.001
velocity all create 300 12345 mom yes rot no
```

```
fix 1 all nvt temp 300 300 100 drag 1
thermo          20
thermo_style custom step temp c_temp_substrate
run 20000
unfix 1
# ---------------------- VISUALIZATION ----------------------------
dump  1 all image 200 output34/image.*.png type type center s 0.5 0.5 0.68 zoom 3.5 axes no 45 0.02 view 90 0
dump_modify 1 backcolor white boxcolor white acolor 1*9 green/red/aqua/yellow/blue/orange/cyan
# dump 2 all cfg 200 output32/dump.Ag_*.cfg mass type xs ys zs id fx fy fz
# dump_modify   2 element Ag
# ---------------------- NCs DEPOSITION ----------------------------
reset_timestep  0
fix 1 all npt temp 300 300 1 iso 0 0 100 drag 1
fix 2 substrate temp/rescale 600 300.0 300.0 1.0 1.0
fix_modify 2 temp temp_substrate
region          NP0 sphere 6.5 6.5 30 6.2
lattice  fcc ${latparam} orient x 1 1 0 orient y -1 1 0 orient z 0 0 1
create_atoms   2 region NP0
group NP0 region NP0
velocity NP0 set 0 0 -8
run 5000
region          NP1 sphere 14 6.5 30 6.2
lattice  fcc ${latparam} orient x 1 1 0 orient y -1 1 0 orient z 0 0 1
create_atoms   3 region NP1
group NP1 region NP1
velocity NP1 set 0 0 -8
run 5000
region          NP2 sphere 6.5 17 30 6.2
lattice  fcc ${latparam} orient x 1 1 0 orient y -1 1 0 orient z 0 0 1
```

```
create_atoms   4 region NP2
group NP2 region NP2
velocity NP2 set 0 0 -8
run 5000
region          NP3 sphere 15 21 30 6.2
lattice  fcc ${latparam} orient x 1 1 0 orient y -1 1 0 orient z 0 0 1
create_atoms   5 region NP3
group NP3 region NP3
velocity NP3 set 0 0 -8
run 5000
region          NP4 sphere 7 9 40 6.2
lattice  fcc ${latparam} orient x 1 1 0 orient y -1 1 0 orient z 0 0 1
create_atoms   6 region NP4
group NP4 region NP4
velocity NP4 set 0 0 -8
run 5000
region          NP5 sphere 15 6.5 40 6.2
lattice  fcc ${latparam} orient x 1 1 0 orient y -1 1 0 orient z 0 0 1
create_atoms   7 region NP5
group NP5 region NP5
velocity NP5 set 0 0 -8
run 5000
region          NP6 sphere 8 20 40 6.2
lattice  fcc ${latparam} orient x 1 1 0 orient y -1 1 0 orient z 0 0 1
create_atoms   8 region NP6
group NP6 region NP6
velocity NP6 set 0 0 -8
run 5000
region          NP7 sphere 16 23 40 6.2
lattice  fcc ${latparam} orient x 1 1 0 orient y -1 1 0 orient z 0 0 1
create_atoms   9 region NP7
```

```
group NP7 region NP7
velocity NP7 set 0 0 -8
run 5000

# SIMULATION DONE
print "All done"
```

APPENDIX 2: INPUT SCRIPT FOR 3 NM CLUSTER DEPOSITION

The LAMMPS code used to simulate the deposition of 3 nm NCs is detailed below. The substrate is of dimension 30×30×10 lattice units. The deposition rate is fixed by releasing a new NC each 20 ps. The NC velocity is fixed to 800 m/s here. The first thermalization lasts 20 ps, the last one 40 ps. A log file reporting the simulation settings is generated and two different outputs are created, either a .jpg format or .cfg format.

```
# ------------------------ INITIALIZATION ----------------------------
units           metal
dimension       3
boundary        p       p       p
atom_style      atomic
variable latparam equal 4.09

# ----------------------- ATOM DEFINITION ----------------------------
lattice         fcc ${latparam}
region          box block 0 30 0 30 -40 40
create_box      9 box

region          substrate block 0 30 0 30 0 10
lattice  fcc ${latparam} orient x 1 0 0 orient y 0 1 0 orient z 0 0 1
create_atoms   1 region substrate
group substrate region substrate

# ------------------------ FORCE FIELDS ------------------------------
pair_style      eam/alloy
pair_coeff      * * Ag.eam.fs Ag Ag Ag Ag Ag Ag Ag Ag Ag
# ------------------------- SETTINGS ---------------------------------

compute temp_substrate all temp/region substrate
```

```
# ---------------------- THERMALIZATION ----------------------------
reset_timestep 0
timestep 0.001
velocity all create 300 12345 mom yes rot no
fix 1 all nvt temp 300 300 100 drag 1
thermo          20000
thermo_style custom step temp c_temp_substrate
run 20000
unfix 1

# ---------------------- VISUALIZATION ----------------------------
dump   1 all image 200 output53/image.*.png type type center s 0.5 0.5 0.5 zoom 3.5 axes no 45 0.02 view 90 0
dump_modify                1 backcolor white boxcolor white acolor 1*9 green/red/aqua/yellow/blue/orange/cyan
# dump 2 all cfg 5000 output49/dump.Ag_*.cfg mass type xs ys zs id fx fy fz
# dump_modify   2 element Ag

# ---------------------- NCs DEPOSITION ----------------------------
reset_timestep 0
# fix 1 all nvt temp 300 300 100 drag 1
fix 1 all npt temp 300 300 1 iso 0 0 100 drag 1
fix 2 substrate temp/rescale 100 300.0 300.0 1.0 1.0
fix_modify 2 temp temp_substrate

region          NP0 sphere 4.75 4.75 15 3.7
lattice  fcc ${latparam} orient x 1 1 0 orient y -1 1 0 orient z 0 0 1
create_atoms   2 region NP0
group NP0 region NP0
velocity NP0 set 0 0 -8
run 20000
```

```
region            NP1 sphere 4.5 11.25 15 3.7
lattice  fcc ${latparam} orient x 1 1 0 orient y -1 1 0 orient z 0 0 1
create_atoms   3 region NP1
group NP1 region NP1
velocity NP1 set 0 0 -8
run 20000

region            NP2 sphere 11.25 4.5 15 3.7
lattice  fcc ${latparam} orient x 1 1 0 orient y -1 1 0 orient z 0 0 1
create_atoms   4 region NP2
group NP2 region NP2
velocity NP2 set 0 0 -8
run 20000

region            NP3 sphere 11.25 15 15 3.7
lattice  fcc ${latparam} orient x 1 1 0 orient y -1 1 0 orient z 0 0 1
create_atoms   5 region NP3
group NP3 region NP3
velocity NP3 set 0 0 -8
run 20000

region            NP4 sphere 4.75 10 20 3.7
lattice  fcc ${latparam} orient x 1 1 0 orient y -1 1 0 orient z 0 0 1
create_atoms   6 region NP4
group NP4 region NP4
velocity NP4 set 0 0 -8
run 20000

region            NP5 sphere 11.25 4.75 20 3.7
lattice  fcc ${latparam} orient x 1 1 0 orient y -1 1 0 orient z 0 0 1
```

```
create_atoms   7 region NP5
group NP5 region NP5
velocity NP5 set 0 0 -8
run 20000

region          NP6 sphere 13 17 20 3.7
lattice  fcc ${latparam} orient x 1 1 0 orient y -1 1 0 orient z 0 0 1
create_atoms   8 region NP6
group NP6 region NP6
velocity NP6 set 0 0 -8
run 20000

region          NP7 sphere 4.75 13.25 20 3.7
lattice  fcc ${latparam} orient x 1 1 0 orient y -1 1 0 orient z 0 0 1
create_atoms   9 region NP7
group NP7 region NP7
velocity NP7 set 0 0 -8
run 40000
# SIMULATION DONE
print "All done"
```

References

[1] J. P. Wilcoxon and B. L. Abrams , "Synthesis, structure and properties of metal nanoclusters", Chem. Soc. Rev., 2006,35, 1162-1194

[2] A. N. Sirenko, D. K. Belashchenko, "Thermodynamic properties of silver nanoclusters", Inorganic Materials, April 2012, Volume 48, Issue 4, pp 332-336

[3] Olivier Carton *et al.*, "Optical Characterization of Porous Sputtered Silver Thin Films", Journal of Spectroscopy, Volume 2013 (2013)

[4] P. Zhao, W. Su, R. Wang, X. Xu, and F. Zhang, "Properties of thin silver films with different thickness," Physica E, vol. 41, no. 3, pp. 387–390, 2009.

[5] Esmaeil Zaminpayma et al., "A Study About Nanocluster Deposition of Thin-film Formation by Molecular Dynamics Simulation", Journal of Cluster Science, December 2008, Volume 19, Issue 4, pp 623-629

[6] K. Mirabbaszadeh *et al.*, "Large-Scale Molecular Dynamics Simulations of Energetic Ni Nanocluster Impact onto the Surface", J Clust Sci (2008) 19:411–419

[7] H. Haberland, Z. Insepov, M. Moseler "Molecular-dynamics simulation of thin-film growth by energetic cluster impact", Phys. Rev. B 51, 11061 – Published 15 April 1995

[8] Oliver Rattunde, "Surface smoothing by energetic cluster impact", Journal of Applied Physics 90, 3226 (2001)

[9] K. Nordlund, T.T. Järvi, K. Meinander, J. Samela, Cluster ion–solid interactions from meV to MeV energies, Appl. Phys. A 91, 561–566 (2008)

[10] W. Harbich, in: K.H. Meiwes-Broer (Ed.), Metal Clusters at Surfaces, Springer, Berlin, 2000.

[11] K. Gleason, "Engineering Nanocomposite Polymer Membranes for Olefin/Paraffin Separation", Dissertation, The University of Texas at Austin (2011)

[12] M. Nahar, "Highly Conductive, Nanoparticulate Thick Films Processed at Low Processing Temperatures", Dissertation, The University of Texas at Austin (2012)

[13] G. Noiseau, "Film deposition and mechanical properties of silver produced by impaction of nanoparticles", Thesis, The University of Texas at Austin (2012)

[14] C. Huang, W.T. Nichols, D.T. O'Brien, M.F. Becker, D. Kovar et al. (2007) Supersonic jet deposition of silver nanoparticle aerosols: Correlations of impact conditions and film morphologies, J. Appl. Phys. 101, 064902 (2007)
[15] M. Nahar *et al.,* Metal-on-oxide nanoparticles produced using laser ablation of microparticle aerosols, Journal of Nanoparticle Research (2011)
[16] W. T. Nichols, J. W. Keto, D. E. Henneke, J. R. Brock, G. Malyavanatham, M. F. Becker, and H. D. Glicksman , "Large-scale production of nanocrystals by laser ablation of microparticles in a flowing aerosol", Applied Physics Letters 78, 1128 (2001)
[17] William T. Nichols, Gokul Malyavanatham, Dale E. Henneke, James R. Brock, Michael F. Becker,John W. Keto and Howard D. Glicksman, "Gas and pressure dependence for the mean size of nanoparticles produced by laser ablation of flowing aerosols", Journal of Nanoparticle Research 2: 141–145, 2000.
[18] Mark E. Tuckerman, "Understanding Modern Molecular Dynamics: Techniques and Applications", J. Phys. Chem. B, 2000, 104 (2), pp 159–178
[19] J. Hansen, " Dynamics of Colloidal Systems: Beyond the Stochastic Approach", NATO Science Series Volume 371, 2002, pp 1-16
[20] D. Frenkel and B. Smit. Understanding Molecular Simulation: From Algorithms to Applications. Academic Press, 2002
[21] S. M. Foiles, M. I. Bakes, and M. S. Daw (1986). Embedded-atom-method functions for the fcc metals Cu, Ag, Au, Al, Pd, Pt, and their alloys. Phys. Rev. B 33, 7893–7991.
[22] Doyama, M. and Kogure, Y., Embedded Atom Potentials in fcc and bcc Metals, Comput. Mater. Sci., 1999, vol. 14, pp. 80–83
[23] S. J. Plimpton, 1995 Fast Parallel Algorithms for Short-Range Molecular Dynamics, J. Comp. Phys. 117 1-19; http://lammps.sandia.gov
[24] S. J. Plimpton and A. P. Thompson 2012 Computational aspects of many-body potentials, MRS Bulletin 37 513-521
[25] S. Plimpton, LAMMPS user's manual, Sandia National Laboratory, (2005)
[26] Ju Li, "AtomEye: an efficient atomistic configuration viewer", Modelling Simul. Mater. Sci. Eng. 11 (2003) 173–177 PII: S0965-0393(03)57873-1
[27] Handbook of The Elements and Native Oxides, B. Vincent Crist, XPS International, Inc., 1999

[28] K. Meinander, T. Claub, and K. Nordlund, "Deposition energy dependence in cluster-assembled thin film densities", Mater. Res. Soc. Symp. Proc. Vol. , 2006

Vita

Nawel Boumerdassi was born in Algiers, Algeria, in 1989. She graduated with highest honors from Lycée Jean-Baptiste-Say in Paris, France, in 2007. She pursued her undergraduate studies enrolling in Classes Préparatoires aux Grandes Ecoles-CPGE at Lycée Janson de Sailly in Paris, France. From 2007, Nawel spent three years in the intensive undergraduate preparation for the national entrance examinations to French engineering colleges. She was admitted in Ecole Centrale de Lille in 2010 and obtained her bachelor of Science in Engineering in May 2014. She enrolled in 2012 to pursue a Master of Science in Electrical and Computer Engineering under the supervision of Dr. Michael F. Becker.

Email address: nawel.boumerdassi@utexas.edu
This thesis was typed by Nawel Boumerdassi.